Glacially enhanced silicate weathering revealed by Holocene lake records

Yi Hou[1*], J. Jotautas Baronas[2,3], Preston Cosslett Kemeny[4], Julien Bouchez[2], Áslaug Geirsdóttir[5], Gifford H. Miller[6], Mark A. Torres[1]

[1]Department of Earth, Environmental, and Planetary Sciences, Rice University
6100 Main Street, Houston, TX 77005, United States
[2]Institut de Physique du Globe de Paris (IPGP) - CNRS - Université Paris Cité
1 Rue Jussieu, 75005 Paris, France
[3]Department of Earth Sciences, Durham University
Durham DH1 3LE, United Kingdom
[4]Department of the Geophysical Sciences, The University of Chicago
5801 S Ellis Ave, Chicago, IL 60637, United States
[5]Faculty of Earth Sciences, University of Iceland,
Askja Sturlugata 7, 102 Reykjavík, Iceland
[6]Institute of Arctic and Alpine Research (INSTAAR)
University of Colorado, 4001 Discovery Drive Boulder, CO 80303, United States

[*]To whom correspondence and requests for materials should be addressed; yihou.012559@gmail.com,
current address: Department of Earth and Planetary Sciences, ETH Zürich,
Sonneggstrasse 5, Zürich 8092, Switzerland

Abstract:

How glaciation affects CO_2 drawdown by chemical weathering sets the strength of the weathering-climate feedback, which controls the exogenic carbon cycle and planetary habitability [1]. However, the exact role of glaciers remains elusive as glaciation alters multiple factors controlling weathering, the net effect of which is ambiguous even in directionality. While illustrative, modern observations have limited ability to constrain time-dependent behavior, which is thought to be important to glacial weathering [2, 3]. To isolate and quantify the effect of glaciers over millennial timescales, we developed a novel multi-proxy system for constraining catchment-scale fluxes in the past. This approach utilizes the correlation between Ge/Si and Si isotope ratios in modern rivers, which sensitively tracks weathering processes, and the preservation of these signals in biogenic silica in lake sediments. We report changes in weathering fluxes in two catchments with different glacial histories during the past ten thousand years from two lacustrine records in Iceland. We find that the chemical weathering fluxes are an order of magnitude higher in the same catchment when glaciated compared to when ice free. The synchronous variations in weathering fluxes with the expansion and contraction of glaciers indicate a rapid effect of glaciation that may amplify climatic variations via a positive feedback.

Significance Statement

The directionality, magnitude, and timing of the chemical weathering response to glaciation remains extensively debated. Past work has either compared modern weathering fluxes between currently glaciated and ice-free catchments or relied on marine sedimentary records. To provide new insight, we developed an approach using lake sediment that provides absolute estimates of paleo-weathering fluxes at the same spatial scale as modern rivers. We find that fluxes are higher when a catchment is glaciated, which supports the hypothesis that enhanced weathering is in phase with glacial activity over millennia. Our work also shows that some portions of the land surface do not follow the global negative climate weathering feedback, which may be important in generating multiple steady states in the carbon cycle.

The chemical weathering of silicate minerals is a major geologic source of alkalinity to the ocean-atmosphere system. The climatic dependence of silicate weathering reactions allows for a negative feedback thought to help regulate Earth's climate and habitability over geologic timescales [1, 4]. However, additional controls on silicate weathering exist [5, 6, 7, 8], and understanding these factors is required to accurately assess the weathering-climate feedback. In particular, large uncertainties exist regarding the effects of glaciation on chemical weathering. At temperatures sufficiently low to initiate and sustain glaciation, chemical weathering is expected to be attenuated due to the sluggish kinetics. Conversely, glaciers enhance supply of fresh mineral surfaces available for reaction [9] by efficiently eroding bedrock [10, 11].

Today, catchment-scale weathering fluxes are often inferred from river solute chemistry [12, 13]. However, observations from modern glacial catchments capture only snapshots in time and, essentially, reflect the behavior of glacial systems during the current interglacial period. Moreover, river chemistry in currently non-glaciated catchments can be heavily influenced by landscapes that are still recovering from past glaciation [3], therefore biasing the estimates of non-glacial weathering fluxes. By altering the topography and the supply of weatherable substrates for prolonged periods, the impact of glaciers on chemical weathering may last well beyond deglaciation [9, 2]. As such, isolating the effect of glaciation on chemical weathering requires accounting for the effects of landscape evolution through time.

Marine sedimentary archives have been used to infer secular changes in continental weathering including during glacial/interglacial periods [14, 15, 16, 17]. These inferences, however, cannot be directly compared to modern catchment-scale estimates of weathering fluxes from river chemistry as marine records derived from biogenic/inorganic precipitates integrate chemical weathering processes over sub-continental to global scales. Further, because the land surface is heterogeneous, global integration can blur the signal of weathering response to glaciation *alone*. Besides issues with different scales of spatial and temporal integration, available weathering proxies largely record flux ratios (e.g., weathering intensity) and/or utilize trace elements that can be decoupled from the release of alkalinity during silicate weathering [18, 19, 20]. To address these issues, we

turn to lake sedimentary records instead, to infer paleo-weathering fluxes at the same spatial scale as modern riverine observations. We present the first application of a novel multi-proxy model that constrains absolute changes in chemical weathering fluxes (in mol Si/km^2 yr) back in time in response to (de)glaciation. Leveraging the sensitivity of river dissolved chemistry, i.e. germanium to silicon ratios (Ge/Si) and Si isotope ratios (δ^{30}Si), to silicate weathering processes, our approach utilizes these chemical signatures recorded in biogenic silica (bSi) preserved in lake sediments to estimate chemical weathering fluxes at the catchment scale.

Inferring weathering flux from bSi River and lake water samples and sediment cores were collected from two lakes and the surrounding regions in western and central Iceland (Figure 1A, Methods). The catchment of Haukadalsvatn (HAK) deglaciated $\sim$12 ka and has been ice free throughout the Holocene [21, 22] (Figure 1B, Methods). In contrast, Lake Hvítárvatn (HVT) deglaciated 11 – 10 ka but now drains the Langjökull glacier (Figure 1C, Methods), which only started to grow in the recent past (i.e. between 5.5 – 5 ka). The region was ice-free during the Holocene Thermal Maximum between 8 and 6 ka in the mid-Holocene [23]. The distinct (de)glaciation histories of the two catchments spanning the past 10 ka, the same time period over which sedimentary archives are available, provide a unique opportunity to evaluate the effect of glaciation on chemical weathering in an internally consistent manner.

A significant negative correlation (Pearson correlation coefficient ρ = -0.84, p = 2.1 $\times 10^{-8}$) was observed between Ge/Si and δ^{30}Si of the dissolved loads of two rivers (Figure 2A). High δ^{30}Si (0.67 – 1.47 ‰) and low Ge/Si (0.4 – 1.5 pM/μM) values are observed at the non-glacial catchment of HAK, whereas the glacial rivers at HVT are characterized by lower δ^{30}Si (-0.09 – 0.27 ‰) and higher Ge/Si (2.1 – 2.8 pM/μM). The covariation between Ge/Si and δ^{30}Si primarily tracks the proportion of dissolved Si partitioned into secondary phases [24, 25] as empirical evidence suggests preferential uptake of Ge and the lighter Si isotopes associated with the formation of secondary phases [26]. Other factors that may alter the riverine Ge/Si and δ^{30}Si compositions [27, 28] can be ruled out – Iceland is virtually monolithologic (volcanic bedrock), sparsely vegetated, and

δ^{18}O and δD measurements of river water from our study sites indicate minimal hydrothermal inputs (Methods, Supplementary Figure 1). Therefore, it appears that the degree of Si uptake into secondary phases, manifested in the co-evolution of solute Ge/Si and δ^{30}Si signatures, is strongly modulated by glaciation (Supplementary Text S4). This is also consistent with previous observations that δ^{30}Si of dissolved loads decreases with increasing glacial cover [29, 30]. Utilizing this empirical correlation between riverine Ge/Si and δ^{30}Si and the expected decoupling between these two tracers during incorporation in biogenic silica, we can infer chemical weathering fluxes in the past from the compositions of diatoms preserved in lake sediments (Figure 2B).

Lake Ge/Si and δ^{30}Si compositions should represent an integrated signal of chemical weathering upstream and fall on the regression line defined by the river data within uncertainties (Figure 2B), which we observe to be true (Figure 2A). The lake chemistry is in turn preserved in the opaline frustules of lacustrine diatoms – these siliceous algae are considered to faithfully record the Ge/Si ratios of the water they grow in [31, 32, 33] and express a Si isotope fractionation according to the degree reflecting nutrient (dissolved Si) utilization [34, 35, 36]. As the initial lake δ^{30}Si at the time of diatom growth can be determined from the Ge/Si ratio recorded in bSi and the empirical correlation between Ge/Si and δ^{30}Si in rivers, the degree of nutrient utilization can be calculated using empirically constrained fractionation factors [37, 38] and the offset between δ^{30}Si of the lake and of preserved diatoms (Eq. 1). The total supply of dissolved Si to the lake, which is effectively the chemical weathering flux in terms of Si, can therefore be computed from the bSi burial flux and the degree of nutrient utilization (Eq. 2). Details on the implementation of this proxy model and the propagation of uncertainties are described in Methods.

$$\underbrace{\delta^{30}\mathrm{Si}_{\mathrm{bSi}}}_{\substack{\text{measured}\\ \text{diatom}}} = \underbrace{\delta^{30}\mathrm{Si}_{\mathrm{initial}}}_{\substack{\text{inferred from Ge/Si-}\\ \delta^{30}\text{Si correlation}}} + \underbrace{\varepsilon}_{\substack{\text{fractionation}\\ \text{factor}}} \cdot \underbrace{f}_{\substack{\text{fraction of}\\ \text{Si remaining}}} \tag{1}$$

$$f = \frac{\text{weathering flux - bSi burial flux}}{\text{weathering flux}} \tag{2}$$

Central to our approach is the assumption that the *correlation* between riverine Ge/Si and δ^{30}Si compositions remained relatively the same in the past 10 ka, i.e. the apparent sensitivity

of riverine Ge/Si and δ^{30}Si to the balance between primary mineral dissolution and secondary mineral formation did not vary. While it is currently not possible to validate this assumption with direct observation, we argue that it is a realistic approximation as the dominant controls on the *style* of chemical weathering (i.e. climatic and tectonic conditions) remained roughly constant during this time period [39]. Another premise of our proxy model regards the absence of post-depositional alteration of Ge/Si and δ^{30}Si of bSi and minimal bSi dissolution. This is corroborated by calculations of diffusive Si fluxes with reactive transport modeling based on the porewater profiles of surface cores (Methods). Further, previous work supports the lack of meaningful Si isotope fractionation during diatom dissolution [40].

At HAK, little variation was observed in Ge/Si (0.5 – 1.0 pM/μM) and δ^{30}Si (-0.86 – -0.39 ‰) of bSi over time, contrary to the wider range of values (Ge/Si: 0.2 – 1.6 pM/μM; δ^{30}Si: -1.28 – -0.40 ‰) measured in bSi at HVT (Figure 2A, 3A, 3B). An unexpected offset between the Ge/Si of core-top bSi and the lake water at HVT is noted (Figure 2A, 3B). We attributed this unexpected biological fractionation of Ge/Si observed at HVT but not at HAK to the difference in lake diatom assemblages (i.e. dominated by planktic vs. benthic species due to different lake turbidity [41]). This fractionation was corrected for in the chemical weathering flux calculations according to the diatom assemblages previously characterized through the core [41] (Methods). Sensitivity tests on this correction suggest that our results and conclusions do not hinge on the specific assumptions on Ge fractionation during diatom growth (Supplementary Text S6, Supplementary Figure 11). However, it is also worth noting that the authors are not aware of any existing work that has systematically examined the Ge uptake behavior of *freshwater* diatoms.

Silicate weathering promoted by glaciers The inferred chemical weathering fluxes (i.e. chemical denudation rates of Si) are presented in Figure 3D and compared against bSi burial fluxes (Figure 3C), which are calculated from previously published sedimentary bSi content and sedimentation rates [22] (Supplementary Text S5). Our lake-derived estimates agree within uncertainties with the weathering fluxes estimated for other watersheds (n = 85) in Iceland from compiled river

chemistry [13] (Figure 4A). Our estimates do appear to be on the higher end of the weathering flux distribution derived from river chemistry, which may reflect substantial groundwater contribution in addition to surface runoff [42]. Groundwater discharge can be important in the Si budget/water mass balance of lakes [35] and is implicitly accounted for in our approach.

At core top, the inferred chemical weathering flux, representative of chemical weathering flux at present, is almost an order of magnitude higher in the glacial catchment than the non-glacial catchment (Figure 3D, 4A). In addition, from the weathering fluxes estimated from compiled Icelandic river chemistry, we found the average of the non-glacial rivers ($3.5\text{x}10^5$ mol Si/km^2/yr, n = 38) to be lower than, or at least comparable to, given the potential uncertainties, the average of glacial rivers (7.3×10^5 mol Si/km^2/yr, n = 9) excluding the multi-source rivers (Figure 4A). These results are contrary to the previous global observation that *"silica denudation rates are distinctly lower in glacier-covered catchments than in their nonglacial counterparts"* [9]. One possible explanation for this discrepancy is that existing global compilations primarily include rivers that drain metamorphic bedrocks whereas volcanic/basaltic lithologies are underrepresented [9]. If true, this points to the potentially *unique* role of glaciation in basalt weathering. Despite its rare occurrence at Earth's surface today [43], basalt plays a disproportional role in atmospheric CO_2 sequestration due to fast dissolution kinetics [12] and its response to glaciation may therefore bear important implications for the carbon cycle.

The first-order changes in chemical weathering fluxes over time share similar patterns with the bSi burial fluxes (Figure 3C, 3D) due to the lack of drastic variation in the degree of nutrient utilization through time (Supplementary Figure 2). At HAK (non-glacial), chemical weathering fluxes remained relatively constant over the past 10 ka (Figure 3D), and a Mann–Kendall statistical test (non-parametric trend detection) cannot reject the null hypothesis that no trend in weathering fluxes exists (Methods). At HVT (glacial), greater variation in chemical weathering fluxes is observed and changes appear non-monotonic in time (Figure 3D). Specifically, the extent of glaciers exerts a strong control on the chemical weathering flux at HVT [44] (Figure 3D, 3E), where higher flux corresponds to larger extents of glaciation (Figure 4B) and more glacial discharge into the lake

(Figure 4C). In addition, we evaluated the completeness of the lake sedimentary records with the previously published age models and concluded that the observed (lack of) trends were robust and did not arise due to sediment preservation bias (i.e. the Sadler Effect [45], Supplementary Text S1, Supplementary Figure S3).

Among currently glaciated watersheds, a slight decrease in the total chemical denudation rates with the increase in the percentage of glacial cover (up to 35 $\%$) was previously observed in south-west Iceland [46]. However, this negative correlation is inconclusive as superimposed effects from the difference in rock ages may be present [46, 10]. Alternatively, our approach affords an interpretation of the variations in chemical weathering fluxes over time primarily in terms of glacial influence and under invariance of other factors, as the evolution of a single catchment is monitored through time. Our results are therefore more representative of the true sensitivity of chemical weathering to the growth and retreat of glaciers.

As mentioned earlier, glaciation may promote chemical weathering through elevated erosion rates. Mechanical erosion rates of 16 – 55.8 t/km^2/yr ($\sim$ 0.06 – 0.2 mm/yr) have been estimated for watersheds adjacent to HAK [47]. Interpolating from the observed correlation between physical erosion and the percentage of glacial cover from the same study, up to two orders of magnitude of increase in erosion rates at HVT between ice-free conditions and the current state may be expected. Indeed, at HVT, the estimated average erosion rates integrated over the Holocene (low average glacial cover) from lake sediment deposits (0.01 – 0.05 mm/yr) [48] are much slower than modern (high glacial cover) denudation rates estimated from river suspended load (0.49 mm/yr) [10].

Implications for the carbon cycle The observed response of chemical weathering to glaciation (Figure 3D, 3E, 4B) contrasts to the hypothesis that the weathering effect temporally lags peak glaciation due to the continued weathering of reactive glacial sediment [2]. Our observation that absolute weathering fluxes are higher in the glaciated catchment further suggest that active glacial processes are more effective at elevating weathering rates compared to the reaction of relic glacial deposits (Figure 3D, 3E, 4). We would like to note that we do not observe a decay in silicate

weathering fluxes at HAK (non-glacial) as predicted by age-dependent weathering rates [2], although the catchment retains deposits of glacial sediment from recent deglaciation ($\sim$10 ka) [49]. It is also possible that a decay of a small magnitude exists but is unresolvable with the uncertainties associated with our estimates.

The positive correlation between silicate weathering and glaciation we observe (Figure 4) suggests that portions of land surface do not necessarily follow global predictions of a negative climate-weathering feedback. This also implies the effects of erosion and runoff as controls for chemical weathering [6, 8], both of which are increased for temperate glaciers [9, 50, 51], can outweigh the temperature dependence [52]. Though the integrated response might be reflective of a negative feedback, individual catchments may be independent and display a wider range of behaviors, in some cases, act to amplify climatic variations. Heterogeneity in the response to climate change may be important in generating multiple steady states in the climate system (i.e., greenhouse and icehouse conditions) and the carbon cycle. While the type of behavior we observe in these two small catchments is not necessarily direct evidence, it represents a plausible mechanism giving rise to bi-stability, which could be further tested via additional study.

Here we presented a new framework that allows the inference of catchment-scale chemical weathering fluxes from terrestrial sedimentary archives, which is powerful because it returns absolute weathering fluxes for Si – one of the major elements involved in silicate weathering – in an analogous manner to observations from modern river systems. As siliceous organisms are widespread in lake systems [34], our approach may be widely adopted to assess and quantify the effects of different environmental controls on chemical weathering.

Methods

Study sites. Haukadalsvatn (HAK, 65.05°N, 21.63°W) is a small lake (3.3 km^2) located in the glacially carved valley of Haukadalur in western Iceland. The meandering Efri Haukadalsá River flows through the valley and drains into Haukadalsvatn. The region is far from the active volcanic zones of Iceland [53] and hydrothermal inputs are therefore expected to be negligible. The 172

km^2 catchment, underlain by Tertiary basalts, has been glacier-free since ∼12 ka. The valley of Haukadalur was briefly submerged at the onset of deglaciation and the basin became isolated from the sea about 10.6 ka [54, 21]. The mean annual temperature of the region is 3.9 ºC (1993 – 2022), according to a weather station (Ásgarður) ∼21 km from the lake (Icelandic Meteorological Office). The valley is currently vegetated by grass and sedges, despite historical accounts describing it as originally largely forested.

Hvítárvatn (HVT, 64.64°N, 19.84°W) is a proglacial lake (28.9 km^2) located on the east side of Langjökull ice cap in central Iceland. Approximately one-third of the watershed (total area: 820 km^2) is now covered by the glacier. However, interpretations of sedimentary deposits and a numerical ice-sheet model reconstruction suggest the extensive advance of Langjökull only began some time between 5 – 3 ka, reaching the maximum extent during the Little Ice Age some 200 years ago, and the region was nearly ice-free in the mid-Holocene after the 8.2 ka cold event [44]. The bedrock in the surrounding area consists primarily of early Holocene lava flows and late Pleistocene subglacial volcanics [55]. A weather station (Hveravellir, ∼30 km from HVT) recorded a mean annual temperature of -0.87 ºC from 1966 to 2003 (Icelandic Meteorological Office). Existing sediment cores dated back to 10 ka from HAK and HVT have been extensively analyzed. Continuous, high-resolution paleoenvironmental records from a variety of physical/chemical proxies have been generated and interpreted in the context of Holocene environmental changes [56, 23, 57, 21, 22, 39].

Sample collection. River and lake water samples in the catchments of Haukadalsá and Hvítá were collected during field campaigns in 2016, 2019, and 2022. Sediment samples from the two lake cores (GLAD4-HAK03-1B, GLAD4-HVT03-1A) were sampled at Institute of Arctic and Alpine Research at University of Colorado, Boulder, and requested from the Continental Scientific Drilling Facilities at the University of Minnesota, respectively. Three additional lake cores (40 – 100 cm) were collected with a vibra-corer (SDI) at Haukadalsvatn in 2022. Coring was planned for Hvítárvatn but was canceled due to inclement weather during the 2022 field season. Water samples were collected for dissolved chemistry 1) directly with single-use 60 mL polypropylene syringes

and filtered through 0.2 μm Polyethersulfone (PES)/nylon/nitrocellulose mixed ester (MCE) syringe filters; 2) with a Van Dorn sampler and subsequently filtered through 0.2 μm MCE/PES filters with a 47 mm filter holder using a peristaltic pump; 3) with a Van Dorn sampler and subsequently filtered through 142 mm 0.2 μm MCE filters with a filtration unit. Several samples were collected in duplicates and no difference in dissolved chemistry was discernible between different filtration methods. Field blanks were collected with filtering deionized water (18.2 MΩ cm^{-1}, referred to here as milliQ) following the same procedures in the field. Water samples were collected in three splits in 1) 50/125 mL polypropylene tubes/bottles, acidified with high-purity nitric acid (HNO3, SCP Science, PlasmaPURE) dispensed from a FEP dropper bottle the day of collection for the analyses of cation and trace element concentrations and isotopes; 2) 2 mL cryovial/15 mL polypropylene tubes for anion concentration and alkalinity measurements; 3) 3 mL exetainers (Labco) with no headspace for water isotope (δ^{18}O and δD) analyses. All sample vials were rinsed three times with the filtered samples before collection. All samples were stored refrigerated except during transportation.

Three sediment cores (40 – 100 cm) were collected on an inflatable boat with a vibracoring device and polycarbonate core liners (9.5 cm inner diameter) at Haukadalsvatn. The core liners were pre-drilled down the length of the core tube and covered with electrical tape before deployment for porewater sampling with Rhizon samplers. Porewaters were extracted from two cores with undisturbed sediment-water interfaces using Rhizon samplers [58] after core retrieval. The Rhizon samplers were inserted every 4 cm top to bottom after draining the overlying water. Porewater samples were stored in 15/50 mL polypropylene and acidified following the same procedures for river water samples.

Separation of biogenic silica from lake sediments. Previously published protocols of density separation and reductive cleaning [59, 60] were followed to purify bSi from the lake sediments. Briefly, 2 – 5 grams of sediment samples were first disaggregated by sonication in $\sim$40 mL 5% sodium hexametaphosphate, rinsed thoroughly with milliQ, and wet-sieved through a 20 μm plastic

sieve. The 20 μm fractions were heated at 90 ºC in a mixture of 10% hydrogen peroxide (H_2O_2) and 1 M hydrochloric acid (HCl) to dissolve organic matter for 5 – 7 hours, during which the solution was carefully decanted and replenished 2 to 3 times to make sure the reactions proceed to completion. Density separation was done with lithium polytungstate ($\sim$2.1 g/cm^3) after the samples were dried on a hot plate (70 ºC). The floating fraction (mostly bSi) was collected, wet sieved again through a 20 μm plastic sieve, thoroughly washed with milliQ, and oven dried at 70 ºC before reductive cleaning. The samples were transferred into clean Teflon beakers (Savillex) and treated with 15 mL of 0.25% hydroxylamine-hydrochloride (NH_2OH-HCl) in glacial acetic acid to remove any metal oxyhydroxide particles. Samples were then etched in 15 mL of 0.1% NaF solution in acidic medium (traces of HCl) for 15 min and treated with a mixture of 7 N HNO_3 and 1.5 N HCl for 2 hours. In between each step, the samples were thoroughly rinsed with milliQ and care was taken to minimize the loss of material. Finally the samples were dried overnight on a hot plate at 70 ºC. Visual and microscopic inspection under an optical microscope suggest no clay particle contamination, which is further corroborated by the low Ge to Si ratios measured for these samples (see Figure 2). Approximately 10 mL of 0.2 M trace-metal clean sodium hydroxide (NaOH) was added to the purified bSi. The samples were placed in the oven (95 ºC) for 24 hours. Once dissolved, the samples were transferred into polypropylene tubes/bottles, diluted with milliQ, and acidified with concentrated HNO_3 for subsequent Ge/Si and Si isotope analyses.

Chemical and isotopic analyses. Si concentrations were determined by either molybdenum Colorimetry [61] with a spectrophotometer (Thermo GENESYS 180) or a quadrupole ICP-MS (Agilent 7900). Measurements of certified reference materials BIGMOOSE-14 (National Research Council Canada), SLRS-6 (National Research Council Canada), and an in-house standard (Mississippi river water) agree with previously reported values. A handful of samples were analyzed with both methods, and the results agree within 5%, which we therefore report as the analytical uncertainty. Ge concentrations were determined by either hydride generation (HG)-ICP-MS on a Triple-Quadruple(TQ)-ICP-MS (Thermo iCAP) with ^{70}Ge isotope spike or analyzed directly with

the TQ-ICP-MS using O_2 as reaction gas in TQ mode. The reproducibility of Ge concentration of an in-house standard (Mississippi river water) was within 10% and a reference material (BHVO, sodium hydroxide fused) is within 15% due to matrix effect. We therefore use 10% and 15% as uncertainties for dissolved samples (i.e. rivers and lakes) and bSi samples, respectively. Si and Ge concentrations in the field blanks are below detection limit, indicating minimal contamination during sample collection.

The Si isotopic compositions of the samples were measured during two sessions at the PARI analytical platform of IPGP on a Multi-Collector (MC)-ICP-MS (Thermo Neptune/Neptune Plus) following previously published methods [62]. Briefly, chromatographic separation of Si was done with cation exchange using AG50W-X12 resin (200 – 400 mesh, BioRad). Between 0.6 and 5 mL of sample was loaded onto the column, eluted with milliQ to obtain a final Si concentration of 1 – 2 ppm, and acidified to a final HNO_3 concentration of 0.1 N. The mass spectrometer was operated in medium resolution. Measurements of samples were bracketed with concentration-matched NBS-28 standard (NIST) prepared using the same cation exchange methods and each sample was measured in 4 replicates. Typical signal intensity was $\sim$5 V for ^{28}Si at 1 ppm while the blank was less than 40 mV. Several reference materials (Diatomite, BHVO, BCR, BIR) and an in-house standard (Mekong river water) were measured multiple times, all of which agree with previously published values. Moreover, mass-dependent fractionation following expected relationships was verified for each analysis session. The measurement uncertainty is reported as the internal 2σ standard error of sample replicates, or 2σ standard deviation of measurements of all reference materials/standard within a given analytical session, whichever is higher.

Oxygen and hydrogen isotopes (δ^{18}O, δD) of river water samples were measured with a cavity ring-down spectrometer (Picarro L2130-i). The precision is 0.1 ‰ for δ^{18}O and 1 ‰ for δD, based on the reproducibility of two reference materials, IA-R064 (Iso-Analytical), USGS47 (RSIL) and two in-house standards.

Si mass balance of the lakes. The benthic diffusive flux of Si driven by the dissolution of biogenic silica (i.e. diatom frustules) was estimated with two porewater profiles at Haukadalsvatn (Supplementary Figure 4). At steady state, the porewater Si concentration C_z at depth (z) can be parameterized with the following equation [63]:

$$C_z = C_d - (C_d - C_0) \cdot \exp(-\beta \cdot z) \tag{3}$$

where C_d is the asymptotic Si concentration when depth approaches infinity, C_0 is the Si concentration at the water-sediment interface, and β describes the attenuation of dissolution with depth. Each of the porewater profiles was fitted with Equation 3, and the diffusive flux was subsequently calculated with Fick's first law:

$$J = -\phi^3 \cdot D \cdot (\frac{dC}{dz})_0 \tag{4}$$

where ϕ is the coretop sediment porosity (0.8, measured by wet/dry weight difference from a separate core), D is the molecular diffusivity of silicic acid in water (2.2×10^{-5} cm^2/s, [64]), and $(\frac{dC}{dz})_0$ is the Si concentration gradient at the water-sediment interface (calculated with the fitted parameters in Equation 3). The tortuosity effect on diffusivity was incorporated by the term ϕ^3 [65]. The calculated diffusive fluxes are 0.025 and 0.057 mol Si/m^2/yr, respectively from the two cores. On average, the magnitude of diffusive flux is less than 1% of the modern bSi burial flux at HAK. As we were not able to collect a surface sediment core at HVT, there is no direct constraints on the benthic fluxes in the glacial lake. However, given the comparable bSi contents in the sediments, bSi burial fluxes, and dissolved Si concentrations in the two lakes, we speculate the dynamics of benthic Si cycling are similar between HAK and HVT, where the dissolution of bSi is limited and the recycling flux is negligible compared to the burial flux.

Residence time of Si in the lakes. To constrain the dynamics of Si cycling in the lakes and assess the timescale over which a change in chemical weathering will be reflected in the lake chemistry and subsequently buried diatoms, the residence time of Si in each lake was calculated as follows.

At steady state, the residence time of Si in each lake τ can be calculated with Equation 5.

$$\tau = \frac{M_{\text{Si}}}{Q_{\text{outflow}} + Q_{\text{burial}}} \tag{5}$$

where M_{Si} is the total mass of Si in the lake in both dissolved phase and assimilated in biomass (i.e. living diatoms). Q_{outflow} is the dissolved Si flux at the lake outlet, calculated with discharge data from gauging stations at/near the lake outlet. Q_{burial} is the bSi burial flux calculated with previously published sedimentation rate and biogenic silica content with a bulk sediment density of 2 g/cm^3 [22]. Lake volume was estimated with lake bathymetry data [21, 41]. A diatom density of 0.14 g/L was assumed for both lakes, which represents the upper limit of the algal biomass density during blooms [66]. Therefore, the estimated residence time should also be considered as an upper limit, which we calculate using Eq. 5 to be less than 1 – 2 years for both lakes. The short residence time of Si in the lakes suggests that any changes in lake chemistry can be recorded by diatoms at high temporal resolution. We further assume that the Si mass balances for the two lakes remained relatively the same during the last 10 kyr as we presently lack independent constraints for Si cycling in the past. However, we argue that this assumption is likely valid because the climate has been relatively stable over this time period (a maximum of 3 ºC above modern temperature during Holocene Thermal Maximum, [39]) and 10 kyr is short on tectonic timescales that basin geometry is unlikely to have been much different.

Weathering flux calculations Measured Ge/Si and Si isotope ratios of river samples were regressed with York regression [67] to account for the uncertainties in both datasets. It is also recognized that the co-evolution of solute Ge/Si and δ^{30}Si as a function of the extent of secondary phase formation can be parameterized as a function Ge/Si and δ^{30}Si of the parent material, and the Ge/Si partition coefficient and Si isotope fractionation factor associated with the formation of secondary phases [25]. However, we opted to use the empirical correlation defined by modern river observations for simplicity and to avoid making further assumptions about poorly constrained parameters. Ge/Si of the lakes in the past can be inferred from measured Ge/Si of the bSi samples as diatoms are considered to record the Ge/Si signatures of the water they grow in [59] except under extreme

nutrient limitations [33]. However, previous work has been focused on marine species, and little is known about the incorporation of Ge into freshwater diatom frustules during growth. At HAK, consistently with expectations we observe no fractionation of Ge/Si between coretop bSi and lake water, implying that diatoms provide a faithful Ge/Si record there. At HVT, an offset between coretop bSi and lake water is observed, suggesting discrimination against Ge during uptake due to different diatom species/communities inhabiting the lake. While the authors are not aware of any existing work that has systematically examined the Ge uptake behavior of freshwater diatoms, the discrimination of Ge during diatom growth agree with previous observation made at the Lower Kern river [24]. In addition, there appears to be a step change in Ge/Si ratios of the bSi samples with time, where the 3 youngest samples have much lower Ge/Si values. Independent constraints indicate a shift from a benthic-dominated to a pelagic-dominated diatom community during the same time period, most likely due to an increasing supply of sediments and thus turbidity from the expansion of Langjökull glacier between 5 – 3 ka [41] (Supplementary Figure 5). Therefore, an offset from lake Ge/Si could be expected for bSi samples younger than this transition, whereas the older bSi samples should closely record lake Ge/Si, as the diatoms then should share similar Ge and Si uptake pathways as the ones currently inhabiting HAK. It then follows that we apply the observed offset between Ge/Si of modern lake and core-top bSi to the youngest three samples at HVT, while no corrections were made for the older samples (Supplementary Figure 10). Silicon isotope ratios were then calculated with inferred Ge/Si of the lake using this correlation, which should represent the compositions of the lake at the time when the diatoms grew. An open-system model was used for diatom growth as the estimated Si mass balance of the lakes suggest minimal recycling flux from the sediments and the high dissolved concentrations of Si in the lake are likely sustained by sufficient river/groundwater supply (see previous section, Supplementary Text S2, and S3 for details). The expected Si isotope composition of diatoms ($\delta^{30}Si_{bSi}$) can be described with Equation 1 [68, 34, 35], where $\delta^{30}Si_{initial}$ is the initial Si isotope composition of the dissolved Si source to the lake, which is practically the same as $\delta^{30}Si_{lake}$ given the short residence time of Si in the lake (see above); ε is the fractionation factor of freshwater diatoms during Si uptake (–1.1

$\pm$ 0.41 ‰, [37, 38]); f is the fraction of remaining dissolved Si, defined as the ratio between Si concentration after and before diatom production. Because the benthic recycling fluxes of Si are negligible and both lakes are not endorheic, this fraction f also relates the bSi burial flux and the total Si supply to the lake (i.e. the weathering flux, Equation 2). We estimated f with Equation 1 using a Monte Carlo approach to account for the uncertainties associated with the analytical measurements, fitting parameters, and the estimate of the fractionation factor from literature values. Weathering fluxes were then calculated with the degree of nutrient utilization (f) and the bSi burial fluxes.

Statistical Tests. We use the non-parametric Mann-Kendall test to assess whether a monotonic trend is present in the change of weathering fluxes with time at HAK, which allows us to avoid making assumptions about 1) the underlying distribution of the samples, 2) the exact functional form between the weathering flux and time. To account for the uncertainties with the inferred weathering fluxes, we use a Monte Carlo approach. Only 36$\%$ of the resampled time series (N = 1 $\times$ 10^5) reject the null hypothesis that a monotonic trend is present at the significance value of 0.05 (α = 0.05). Therefore, we conclude that there is no statistically significant temporal trend in the reconstructed weathering fluxes at HAK.

Similarly, to test whether there is a significant correlation between weathering fluxes and glacial extent (i.e. ice area and glacial discharge), we resampled the estimated chemical weathering fluxes at HVT to propagate the uncertainties. With a Pearson's correlation test, we found that more than 80 $\%$ of the resampled time series (N = 1 $\times$ 10^5) reject the null hypothesis of no correlation at the significance value of 0.05 (α = 0.05). As such, we conclude that there is a correlation between glacial extent and weathering flux.

Data availability

All data and code generated as part of this study and code for flux calculations will be made public through `Github` and deposited permanently in `Zenodo` upon publication of this manuscript after

peer review.

Acknowledgments

M.A.T. acknowledges support from NSF-EAR 2017106. Y.H. acknowledges support from a Wagoner Foreign Study Scholarship from Rice University. P.C.K. acknowledges support through the T.C. Chamberlin Fellowship at the University of Chicago and through an NSF-EAR postdoctoral fellowship (2204376). We thank Trevor Cole, Will Larsen, Miriam Gammerman, Matthias Walder, and Sam Scott for assistance with field work; Wendy Roth for facilitating sediment core sampling at INSTAAR; Pierre Burckel, Tu-Han Luu, Dimitri Rigoussen, and Sofía López-Urzúa for help with chemical/isotopic analyses at IPGP; Evan J. Ramos for discussions. The work benefited from the IPGP multidisciplinary program PARI and the Region Île-de-France SESAME Grant No. 12015908.

Author contribution

M.A.T. and Y.H. conceived and designed the study. Y.H., P.C.K., and M.A.T, conducted the field work. A.G. and G.H.M. curated lake core samples. Y.H. carried out the formal analyses and wrote the manuscript, with contributions from J.J.B, J.B., P.C.K, and M.A.T. All authors contributed comments and/or revisions to the manuscript.

Competing interest

The authors declare that they have no competing interests.

Figures

Figure 1 Sampling sites. (A) Iceland with indicated locations of the lakes in this study: Haukadalsvatn (HAK) and Hvítárvatn (HVT). Black lines delineate modern ice cover. Data were sourced from Arctic Spatial Data Infrastructure. (B) Haukadalsvatn area with indicated sampling locations of river water (white circles), lake water (white square), and sediment core (red circle). (C) Hvítárvatn area with indicated sampling locations. Black dashed lines indicate the extent of the Langjökull and the Eiríksjökull glacier. Elevation data were sourced from Polar Geospatial Center (ArcticDEM) in EPSG 3413 projection.

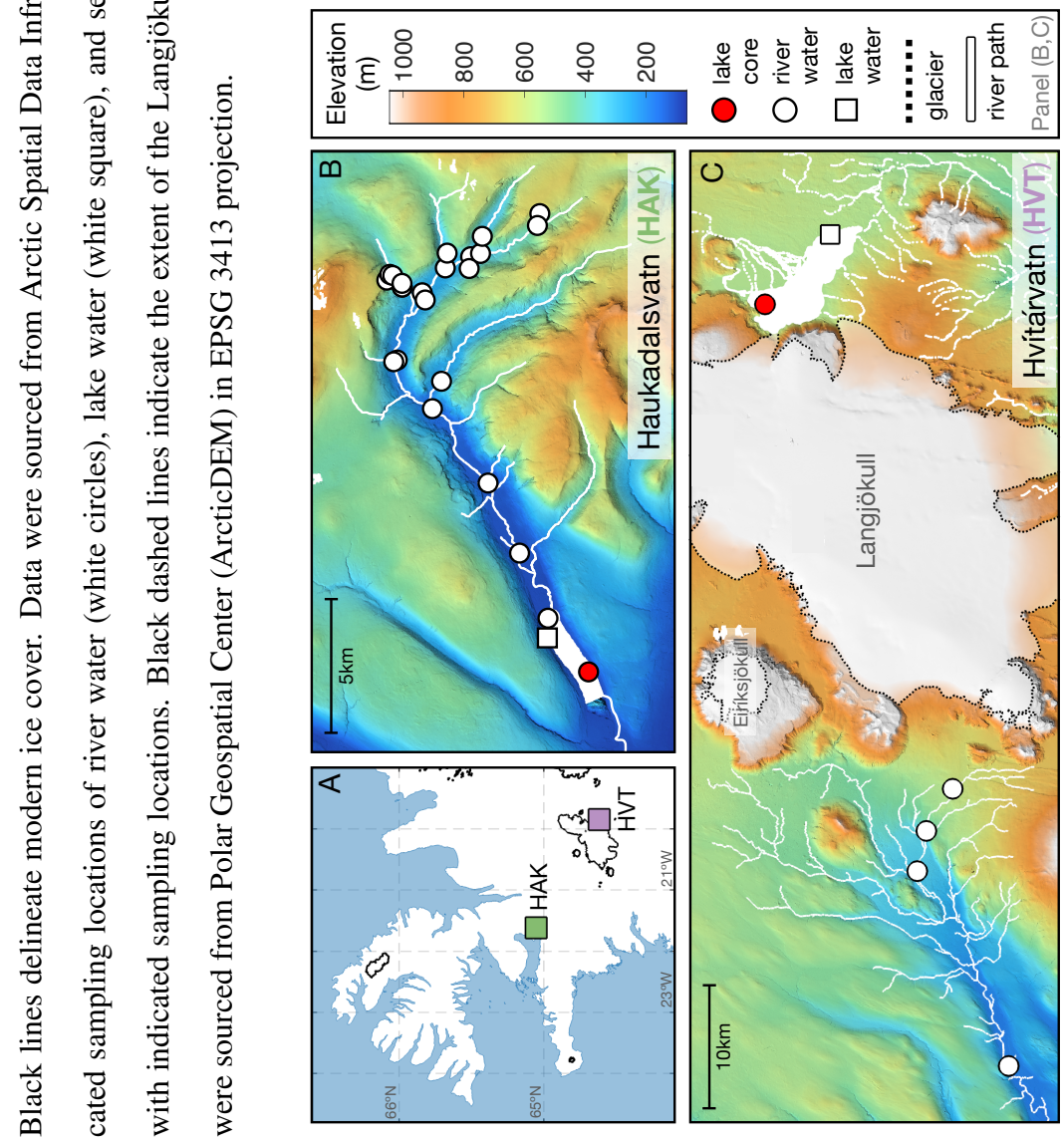

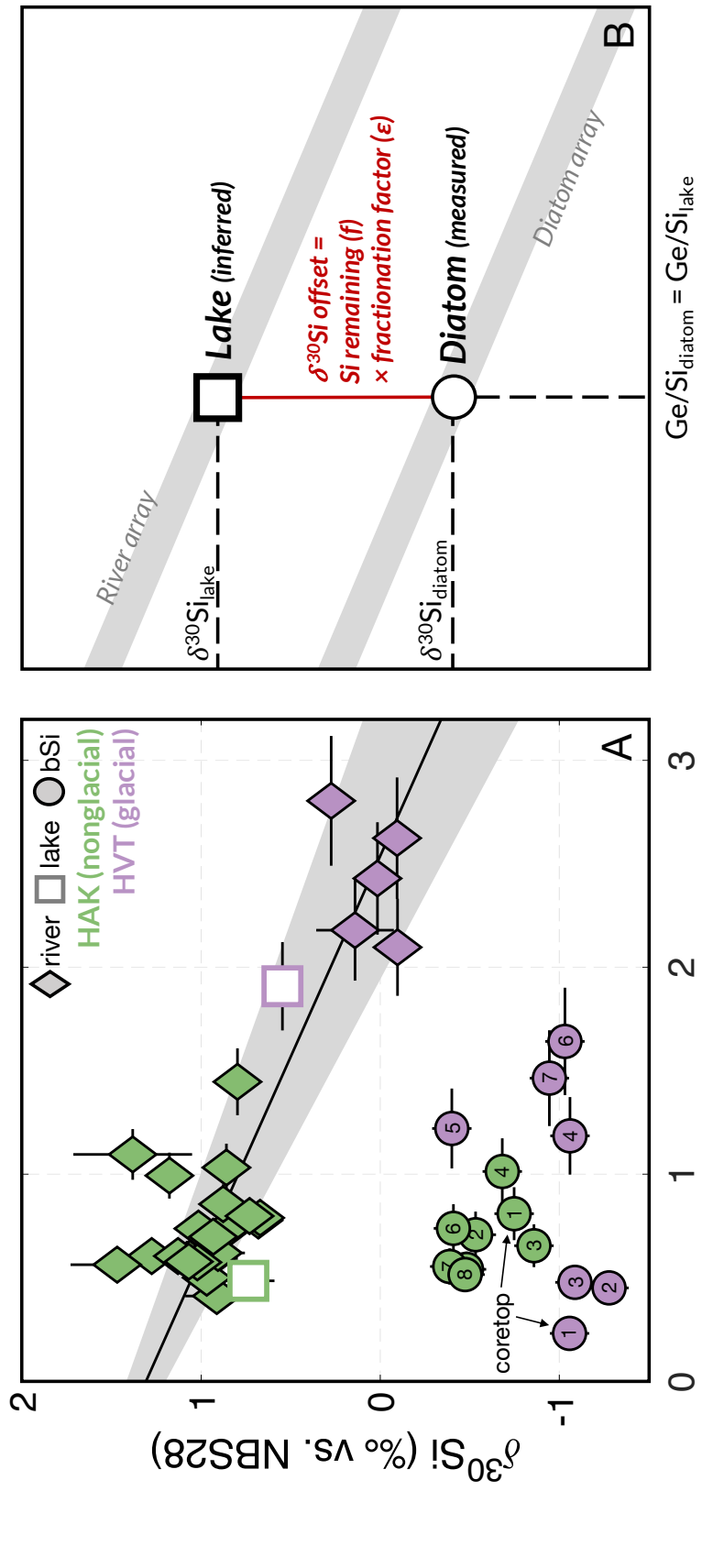

Figure 2 (A) Ge/Si and Si isotope ratios of river water (diamonds), lake water (squares), and biogenic silica (bSi, circles) samples at HAK (nonglacial, green) and HVT (glacial, purple), numbers indicate the relative ages of bSi samples with 1 corresponding to the youngest. δ^{30}Si decreases with increasing Ge/Si in river and lake dissolved load. Offset between δ^{30}Si of bSi and lake water indicate the biological fractionation corresponding to the degree of nutrient utilization by diatoms. (B) Schematic of the proxy model.

Figure 3 (A) Changes in δ^{30}Si of bSi samples over time. (B) Changes in Ge/Si of bSi samples over time. Note the offset between coretop biogenic Si and modern lake water at HVT. (C) Changes in bSi burial flux over time, calculated with previously published sedimentation rate and bSi content with a bulk sediment density of 2 g/cm^3 [22]. (D) Changes in reconstructed chemical weathering fluxes over time. (E) Reconstructed changes in glacial discharge and ice area of Langjökull [44].

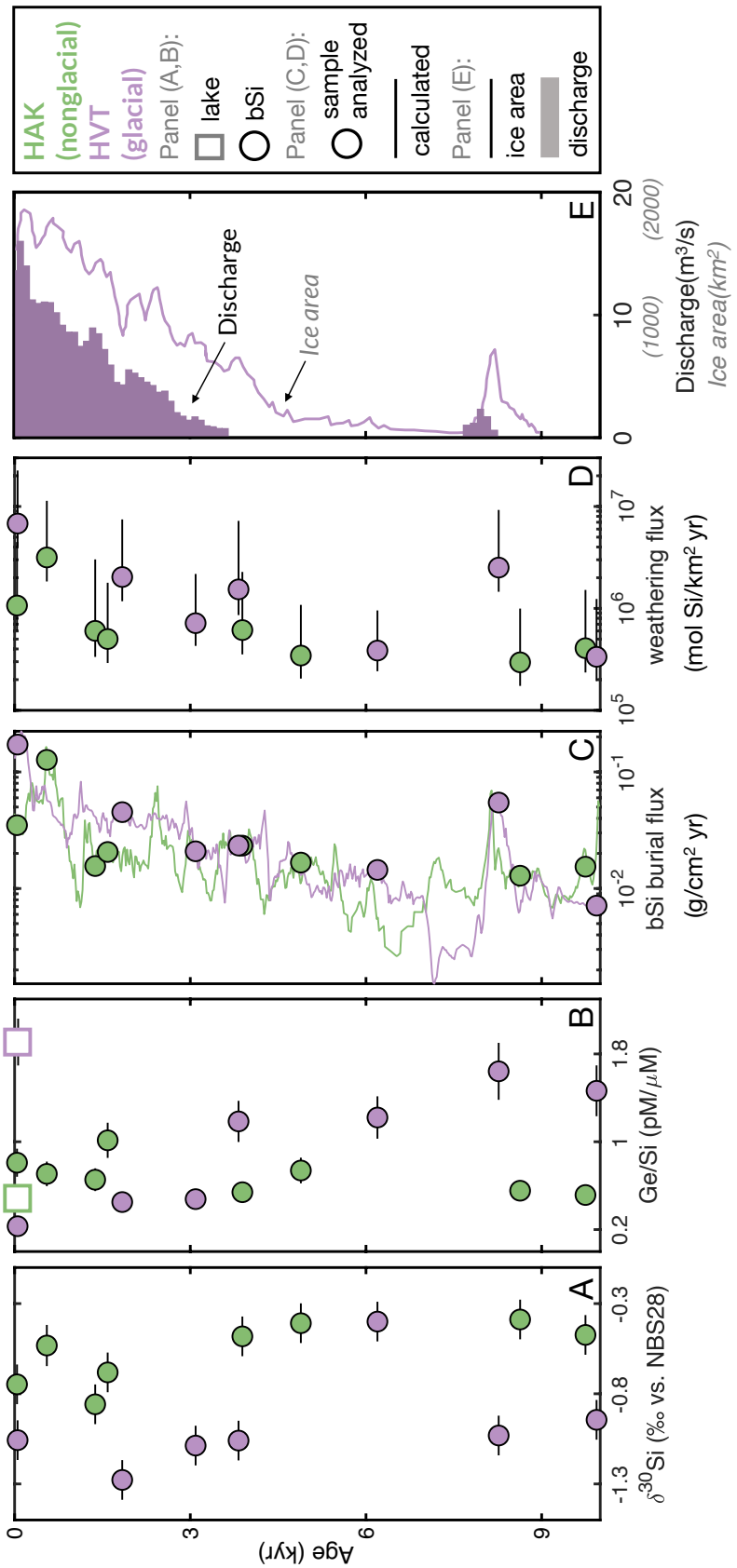

Figure 4 (A) Reconstructed chemical weathering fluxes from bSi are comparable with fluxes estimated from compiled Icelandic river data [13]. (B) Positive correlation between chemical weathering flux at HVT and reconstructed ice extent of Langjökull [44]. (C) Positive correlation between chemical weathering flux at HVT and reconstructed glacial discharge into the lake [44]. The single data point of weathering flux at HAK plotted on Panels (B, C) is the median of the average fluxes over time calculated from resampling of individual inferences (N = 10^5). The error bar corresponds to the range between 10 – 90 percentile.

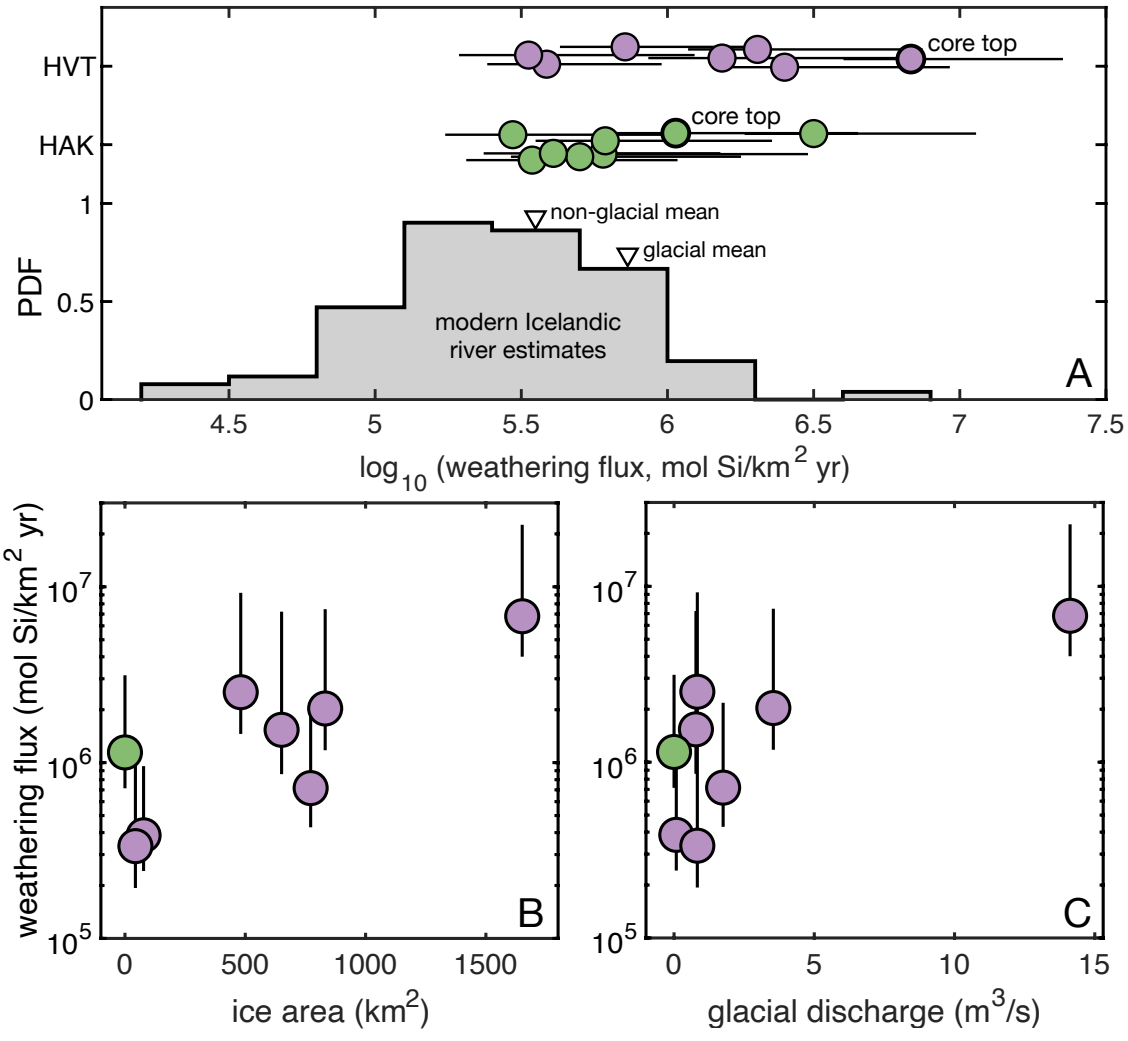

References

[1] L. R. Kump, S. L. Brantley, and M. A. Arthur, "Chemical weathering, atmospheric CO_2, and climate," *Annual Review of Earth and Planetary Sciences*, vol. 28, no. 1, pp. 611–667, 2000.

[2] D. Vance, D. A. Teagle, and G. L. Foster, "Variable Quaternary chemical weathering fluxes and imbalances in marine geochemical budgets," *Nature*, vol. 458, no. 7237, pp. 493–496, 2009.

[3] P. C. Kemeny, M. A. Torres, M. P. Lamb, S. M. Webb, N. Dalleska, T. Cole, Y. Hou, J. Marske, J. F. Adkins, and W. W. Fischer, "Organic sulfur fluxes and geomorphic control of sulfur isotope ratios in rivers," *Earth and Planetary Science Letters*, vol. 562, p. 116838, 2021.

[4] E. S. Eiriksdottir, S. R. Gislason, and E. H. Oelkers, "Does temperature or runoff control the feedback between chemical denudation and climate? Insights from NE Iceland," *Geochimica et Cosmochimica Acta*, vol. 107, pp. 65–81, 2013.

[5] G. J. Bluth and L. R. Kump, "Lithologic and climatologic controls of river chemistry," *Geochimica et Cosmochimica Acta*, vol. 58, no. 10, pp. 2341–2359, 1994.

[6] A. J. West, "Thickness of the chemical weathering zone and implications for erosional and climatic drivers of weathering and for carbon-cycle feedbacks," *Geology*, vol. 40, no. 9, pp. 811–814, 2012.

[7] S. Gudbrandsson, D. Wolff-Boenisch, S. Gislason, and E. Oelkers, "Dissolution rates of crystalline basalt at pH 4 and 10 and 25–75 °C," *Mineralogical Magazine*, vol. 72, no. 1, pp. 155–158, 2008.

[8] K. Maher and C. Chamberlain, "Hydrologic regulation of chemical weathering and the geologic carbon cycle," *Science*, vol. 343, no. 6178, pp. 1502–1504, 2014.

[9] S. Prestrud Anderson, J. I. Drever, and N. F. Humphrey, "Chemical weathering in glacial environments," *Geology*, vol. 25, no. 5, pp. 399–402, 1997.

[10] P. Louvat, S. R. Gislason, and C. J. Allègre, "Chemical and mechanical erosion rates in iceland as deduced from river dissolved and solid material," *American Journal of Science*, vol. 308, pp. 679–726, 5 2008.

[11] F. Herman, D. Seward, P. G. Valla, A. Carter, B. Kohn, S. D. Willett, and T. A. Ehlers, "Worldwide acceleration of mountain erosion under a cooling climate," *Nature*, vol. 504, no. 7480, pp. 423–426, 2013.

[12] C. Dessert, B. Dupré, J. Gaillardet, L. M. François, and C. J. Allègre, "Basalt weathering laws and the impact of basalt weathering on the global carbon cycle," *Chemical Geology*, vol. 202, no. 3-4, pp. 257–273, 2003.

[13] T. L. Cole, M. A. Torres, and P. C. Kemeny, "The hydrochemical signature of incongruent weathering in Iceland," *Journal of Geophysical Research: Earth Surface*, vol. 127, no. 6, p. e2021JF006450, 2022.

[14] G. L. Foster and D. Vance, "Negligible glacial–interglacial variation in continental chemical weathering rates," *Nature*, vol. 444, no. 7121, pp. 918–921, 2006.

[15] G. Henderson, D. Martel, R. O'Nions, and N. Shackleton, "Evolution of seawater $^{87}Sr/^{86}Sr$ over the last 400 ka: the absence of glacial/interglacial cycles," *Earth and Planetary Science Letters*, vol. 128, no. 3-4, pp. 643–651, 1994.

[16] D. E. Hammond, J. McManus, and W. M. Berelson, "Oceanic germanium/silicon ratios: Evaluation of the potential overprint of temperature on weathering signals," *Paleoceanography*, vol. 19, no. 2, 2004.

[17] P. Froelich, V. Blanc, R. Mortlock, S. Chillrud, W. Dunstan, A. Udomkit, and T.-H. Peng, "River fluxes of dissolved silica to the ocean were higher during glacials: Ge/si in diatoms, rivers, and oceans," *Paleoceanography*, vol. 7, no. 6, pp. 739–767, 1992.

[18] M. Dellinger, J. Gaillardet, J. Bouchez, D. Calmels, P. Louvat, A. Dosseto, C. Gorge, L. Alanoca, and L. Maurice, "Riverine Li isotope fractionation in the Amazon River basin controlled by the weathering regimes," *Geochimica et Cosmochimica Acta*, vol. 164, pp. 71–93, 2015.

[19] T. J. Suhrhoff, J. Rickli, K. Crocket, E. Bura-Nakic, and D. Vance, "Behavior of beryllium in the weathering environment and its delivery to the ocean," *Geochimica et Cosmochimica Acta*, vol. 265, pp. 48–68, 2019.

[20] S. Li, S. L. Goldstein, and M. E. Raymo, "Neogene continental denudation and the beryllium conundrum," *Proceedings of the National Academy of Sciences*, vol. 118, no. 42, p. e2026456118, 2021.

[21] Á. Geirsdóttir, G. H. Miller, T. Thordarson, and K. B. Ólafsdóttir, "A 2000-year record of climate variations reconstructed from Haukadalsvatn, West Iceland," *Journal of Paleolimnology*, vol. 41, pp. 95–115, 2009.

[22] Á. Geirsdóttir, G. H. Miller, D. J. Larsen, and S. Ólafsdóttir, "Abrupt Holocene climate transitions in the northern North Atlantic region recorded by synchronized lacustrine records in Iceland," *Quaternary Science Reviews*, vol. 70, pp. 48–62, 2013.

[23] D. J. Larsen, G. H. Miller, Á. Geirsdóttir, and S. Ólafsdóttir, "Non-linear Holocene climate evolution in the North Atlantic: a high-resolution, multi-proxy record of glacier activity and environmental change from Hvítárvatn, central Iceland," *Quaternary Science Reviews*, vol. 39, pp. 14–25, 2012.

[24] J. J. Baronas, M. A. Torres, A. J. West, O. Rouxel, B. Georg, J. Bouchez, J. Gaillardet, and D. E. Hammond, "Ge and Si isotope signatures in rivers: A quantitative multi-proxy approach," *Earth and Planetary Science Letters*, vol. 503, pp. 194–215, 2018.

[25] P. J. Frings, F. Schubring, M. Oelze, and F. von Blanckenburg, "Quantifying biotic and abiotic Si fluxes in the Critical Zone with Ge/Si ratios along a gradient of erosion rates," *American Journal of Science*, vol. 321, no. 8, pp. 1204–1245, 2021.

[26] A. M. Anders, R. S. Sletten, L. A. Derry, and B. Hallet, "Germanium/silicon ratios in the Copper River Basin, Alaska: Weathering and partitioning in periglacial versus glacial environments," *Journal of Geophysical Research: Earth Surface*, vol. 108, no. F1, 2003.

[27] J.-T. Cornelis, B. Delvaux, R. Georg, Y. Lucas, J. Ranger, and S. Opfergelt, "Tracing the origin of dissolved silicon transferred from various soil-plant systems towards rivers: a review," *Biogeosciences*, vol. 8, no. 1, pp. 89–112, 2011.

[28] M. J. Evans and L. A. Derry, "Quartz control of high germanium/silicon ratios in geothermal waters," *Geology*, vol. 30, no. 11, pp. 1019–1022, 2002.

[29] R. Georg, B. C. Reynolds, A. West, K. Burton, and A. N. Halliday, "Silicon isotope variations accompanying basalt weathering in Iceland," *Earth and Planetary Science Letters*, vol. 261, no. 3-4, pp. 476–490, 2007.

[30] H. V. Pryer, J. E. Hatton, J. L. Wadham, J. R. Hawkings, L. F. Robinson, A. M. Kellerman, M. G. Marshall, A. Urra, A. Covey, G. Daneri, *et al.*, "The effects of glacial cover on riverine silicon isotope compositions in Chilean Patagonia," *Frontiers in Earth Science*, vol. 8, p. 368, 2020.

[31] G. Bareille, M. Labracherie, R. A. Mortlock, E. Maier-Reimer, and P. N. Froelich, "A test of (Ge/Si) opal as a paleorecorder of (Ge/Si) seawater," *Geology*, vol. 26, no. 2, pp. 179–182, 1998.

[32] G. M. Filippelli, J. W. Carnahan, L. A. Derry, and A. Kurtz, "Terrestrial paleorecords of Ge/Si cycling derived from lake diatoms," *Chemical Geology*, vol. 168, no. 1-2, pp. 9–26, 2000.

559 [33] J. Sutton, M. J. Ellwood, W. A. Maher, and P. L. Croot, "Oceanic distribution of inorganic
560 germanium relative to silicon: Germanium discrimination by diatoms," *Global Biogeochem-*
561 *ical Cycles*, vol. 24, no. 2, 2010.

562 [34] S. Opfergelt, E. Eiriksdottir, K. Burton, A. Einarsson, C. Siebert, S. Gislason, and A. Hall-
563 iday, "Quantifying the impact of freshwater diatom productivity on silicon isotopes and sil-
564 icon fluxes: Lake Myvatn, Iceland," *Earth and Planetary Science Letters*, vol. 305, no. 1-2,
565 pp. 73–82, 2011.

566 [35] P. Zahajská, C. Olid, J. Stadmark, S. C. Fritz, S. Opfergelt, and D. J. Conley, "Modern silicon
567 dynamics of a small high-latitude subarctic lake," *Biogeosciences*, vol. 18, no. 7, pp. 2325–
568 2345, 2021.

569 [36] K. R. Hendry and M. A. Brzezinski, "Using silicon isotopes to understand the role of the
570 Southern Ocean in modern and ancient biogeochemistry and climate," *Quaternary Science*
571 *Reviews*, vol. 89, pp. 13–26, 2014.

572 [37] C. L. de La Rocha, M. A. Brzezinski, and M. J. DeNiro, "Fractionation of silicon isotopes
573 by marine diatoms during biogenic silica formation," *Geochimica et Cosmochimica Acta*,
574 vol. 61, no. 23, pp. 5051–5056, 1997.

575 [38] L. Y. Alleman, D. Cardinal, C. Cocquyt, P.-D. Plisnier, J.-P. Descy, I. Kimirei, D. Sinyinza,
576 and L. André, "Silicon isotopic fractionation in Lake Tanganyika and its main tributaries,"
577 *Journal of Great Lakes Research*, vol. 31, no. 4, pp. 509–519, 2005.

578 [39] Á. Geirsdóttir, D. J. Harning, G. H. Miller, J. T. Andrews, Y. Zhong, and C. Caseldine,
579 "Holocene history of landscape instability in Iceland: Can we deconvolve the impacts of
580 climate, volcanism and human activity?," *Quaternary Science Reviews*, vol. 249, p. 106633,
581 2020.

582 [40] V. N. Panizzo, G. Swann, A. Mackay, E. Vologina, M. Sturm, V. Pashley, and M. Horstwood,
583 "Insights into the transfer of silicon isotopes into the sediment record," *Biogeosciences Dis-*
584 *cussions*, vol. 12, no. 12, pp. 9369–9391, 2015.

585 [41] J. L. Black, *Holocene climate change in south-central Iceland: A multi-proxy lacustrine*
586 *record from glacial lake Hvítárvatn*. PhD thesis, University of Colorado at Boulder, 2008.

587 [42] H. H. Schopka and L. A. Derry, "Chemical weathering fluxes from volcanic islands and the
588 importance of groundwater: The Hawaiian example," *Earth and Planetary Science Letters*,
589 vol. 339, pp. 67–78, 2012.

590 [43] J. Hartmann and N. Moosdorf, "The new global lithological map database GLiM: A repre-
591 sentation of rock properties at the Earth surface," *Geochemistry, Geophysics, Geosystems*,
592 vol. 13, no. 12, 2012.

593 [44] G. E. Flowers, H. Björnsson, Á. Geirsdóttir, G. H. Miller, J. L. Black, and G. K. Clarke,
594 "Holocene climate conditions and glacier variation in central Iceland from physical modelling
595 and empirical evidence," *Quaternary Science Reviews*, vol. 27, no. 7-8, pp. 797–813, 2008.

596 [45] P. M. Sadler, "Sediment accumulation rates and the completeness of stratigraphic sections,"
597 *The Journal of Geology*, vol. 89, no. 5, pp. 569–584, 1981.

598 [46] S. R. Gislason, S. Arnórsson, and H. Armannsson, "Chemical weathering of basalt in South-
599 west Iceland; effects of runoff, age of rocks and vegetative/glacial cover," *American Journal*
600 *of Science*, vol. 296, no. 8, pp. 837–907, 1996.

601 [47] N. Vigier, K. W. Burton, S. R. Gislason, N. W. Rogers, S. Duchene, L. Thomas, E. Hodge,
602 and B. Schaefer, "The relationship between riverine U-series disequilibria and erosion rates
603 in a basaltic terrain," *Earth and Planetary Science Letters*, vol. 249, no. 3-4, pp. 258–273,
604 2006.

[48] J. Black, G. Miller, Á. Geirsdóttir, W. Manley, and H. Bjornsson, "Sediment thickness and Holocene erosion rates derived from a seismic survey of Hvítárvatn, central Iceland," *Jökull*, vol. 54, pp. 37–56, 2004.

[49] M. A. Torres, P. C. Kemeny, M. P. Lamb, T. L. Cole, and W. W. Fischer, "Long-term storage and age-biased export of fluvial organic carbon: Field evidence from west Iceland," *Geochemistry, Geophysics, Geosystems*, vol. 21, no. 4, p. e2019GC008632, 2020.

[50] M. A. Torres, N. Moosdorf, J. Hartmann, J. F. Adkins, and A. J. West, "Glacial weathering, sulfide oxidation, and global carbon cycle feedbacks," *Proceedings of the National Academy of Sciences*, vol. 114, no. 33, pp. 8716–8721, 2017.

[51] B. Hallet, L. Hunter, and J. Bogen, "Rates of erosion and sediment evacuation by glaciers: A review of field data and their implications," *Global and Planetary Change*, vol. 12, no. 1-4, pp. 213–235, 1996.

[52] J. C. Walker, P. Hays, and J. F. Kasting, "A negative feedback mechanism for the long-term stabilization of Earth's surface temperature," *Journal of Geophysical Research: Oceans*, vol. 86, no. C10, pp. 9776–9782, 1981.

[53] H. Jóhannesson, "Yfirlit um jarðfræði hálendis Mỳrasỳslu og yfir til Dala," *Í fjallhögum milli Mỳra og Dala. Arbók Ferðafélag Íslands, Reykjavık*, pp. 215–226, 1997.

[54] Á. Geirsdóttir, G. H. Miller, Y. Axford, and S. Ólafsdóttir, "Holocene and latest Pleistocene climate and glacier fluctuations in Iceland," *Quaternary Science Reviews*, vol. 28, no. 21-22, pp. 2107–2118, 2009.

[55] J. Sinton, K. Grönvold, and K. Sæmundsson, "Postglacial eruptive history of the western volcanic zone, Iceland," *Geochemistry, Geophysics, Geosystems*, vol. 6, no. 12, 2005.

[56] D. J. Larsen, G. H. Miller, Á. Geirsdóttir, and T. Thordarson, "A 3000-year varved record of glacier activity and climate change from the proglacial lake Hvítárvatn, Iceland," *Quaternary Science Reviews*, vol. 30, no. 19-20, pp. 2715–2731, 2011.

[57] D. J. Larsen, Á. Geirsdóttir, and G. H. Miller, "Precise chronology of Little Ice Age expansion and repetitive surges of Langjökull, central Iceland," *Geology*, vol. 43, no. 2, pp. 167–170, 2015.

[58] J. Seeberg-Elverfeldt, M. Schlüter, T. Feseker, and M. Kölling, "Rhizon sampling of pore-waters near the sediment-water interface of aquatic systems," *Limnology and Oceanography: Methods*, vol. 3, no. 8, pp. 361–371, 2005.

[59] A. Shemesh, R. Mortlock, and P. Froelich, "Late Cenozoic Ge/Si record of marine biogenic opal: Implications for variations of riverine fluxes to the ocean," *Paleoceanography*, vol. 4, no. 3, pp. 221–234, 1989.

[60] J. J. Baronas, D. E. Hammond, W. M. Berelson, J. McManus, and S. Severmann, "Germanium–silicon fractionation in a river-influenced continental margin: The Northern Gulf of Mexico," *Geochimica et Cosmochimica Acta*, vol. 178, pp. 124–142, 2016.

[61] J. Mullin and J. Riley, "The colorimetric determination of silicate with special reference to sea and natural waters," *Analytica Chimica Acta*, vol. 12, pp. 162–176, 1955.

[62] R. Georg, B. C. Reynolds, M. Frank, and A. N. Halliday, "New sample preparation techniques for the determination of Si isotopic compositions using MC-ICPMS," *Chemical Geology*, vol. 235, no. 1-2, pp. 95–104, 2006.

[63] J. McManus, D. E. Hammond, W. M. Berelson, T. E. Kilgore, D. J. Demaster, O. G. Ragueneau, and R. W. Collier, "Early diagenesis of biogenic opal: Dissolution rates, kinetics, and paleoceanographic implications," *Deep Sea Research Part II: Topical Studies in Oceanography*, vol. 42, no. 2-3, pp. 871–903, 1995.

[64] K. R. Applin, "The diffusion of dissolved silica in dilute aqueous solution," *Geochimica et Cosmochimica Acta*, vol. 51, no. 8, pp. 2147–2151, 1987.

[65] W. J. Ullman and R. C. Aller, "Diffusion coefficients in nearshore marine sediments," *Limnology and Oceanography*, vol. 27, no. 3, pp. 552–556, 1982.

[66] R. Ramaraj, D. D.-W. Tsai, and P. H. Chen, "Biomass of algae growth on natural water medium," *Journal of Photochemistry and Photobiology B: Biology*, vol. 142, pp. 124–128, 2015.

[67] D. York, N. M. Evensen, M. L. Martinez, and J. De Basabe Delgado, "Unified equations for the slope, intercept, and standard errors of the best straight line," *American Journal of Physics*, vol. 72, no. 3, pp. 367–375, 2004.

[68] D. E. Varela, C. J. Pride, and M. A. Brzezinski, "Biological fractionation of silicon isotopes in Southern Ocean surface waters," *Global Biogeochemical Cycles*, vol. 18, no. 1, 2004.

Supplementary Information for "Glacially enhanced silicate weathering revealed by Holocene lake records"

Yi Hou[1*], J. Jotautas Baronas[2,3], Preston Cosslett Kemeny[4], Julien Bouchez[2], Áslaug Geirsdóttir[5], Gifford H. Miller[6], Mark A. Torres[1]

[1]Department of Earth, Environmental, and Planetary Sciences, Rice University, 6100 Main Street, Houston, TX 77005, United States
[2]Institut de Physique du Globe de Paris (IPGP) - CNRS - Université Paris Cité, 1 Rue Jussieu, 75005 Paris, France
[3]Department of Earth Sciences, Durham University, Durham DH1 3LE, United Kingdom
[4]Department of the Geophysical Sciences, The University of Chicago, 5801 S Ellis Ave, Chicago, IL 60637, United States
[5]Faculty of Earth Sciences, University of Iceland, Askja Sturlugata 7, 102 Reykjavík, Iceland
[6]Institute of Arctic and Alpine Research (INSTAAR), University of Colorado, 4001 Discovery Drive Boulder, CO 80303, United States
*To whom correspondence and requests for materials should be addressed; E-mail: yihou.012559@gmail.com, current address: Department of Earth and Planetary Sciences, ETH Zürich, Sonneggstrasse 5, NO G6, Zürich 8092, Switzerland

Contents of this file

Text S1: Evaluating the completeness of the sedimentary records The completeness of the lake sedimentary records were assessed to make sure that the presence and lack of temporal trends in the calculated weathering fluxes are not resulted from sediment preservation bias. Due to the internal dynamics in sedimentary systems, sediment rates appear to be lower when integrated over longer timescales due to the incorporation of hiatuses and erosional events in the sedimentary records (referred to as the Sadler effect) [1, 2]. Following the procedures in [2], the changes in sediment thickness between different age control points (ΔH) were plotted against the corresponding changes in time (ΔT) and the logarithms of ΔH and ΔT was regressed (Supplementary Figure 3). Theory predicts that a regressed exponent (β) of 1 means that the sedimentary record is complete, whereas global compilation of observed sedimentation rates yields an exponent of 0.5 [1, 2].

At HVT, the analyses were performed for two segments of the core separately (Supplementary Figure 3 C, D), because 1) the chronology was derived differently above and below the ash layer Hekla 3 (by varve and paleomagnetic secular variation, respectively) [3]; and 2) there is *known* change in the sedimentation rates corresponding to increased glacial discharge into the lake during this time period [4]. The calculated β is very close to 1 in both segments, which suggests that the sedimentary record at HVT is complete and the inferred changes in weathering fluxes did not spuriously arise from sedimentation dynamics.

At HAK, the calculated β is not as close to 1 but still much closer to "completeness" than the global average (β = 0.5 [1]). Previous work has suggested that there's recent ($\sim$1.5 ka) eolian sediment inputs from soil erosion [5] into the lake. We therefore argue that the apparent faster sedimentation rate in younger sediments ($\beta <$1) at HAK is not due to preservation bias but a physical mechanism that changed the sediment supply, and the sediment core at HAK also preserves a faithful record.

Text S2: Constraining the dynamics of Si cycling in the lakes. To constrain how much the system can deviate from a *truly* open system due to seasonality in discharge and diatom growth, a model is constructed as follows with a list of relevant variables specified in Table S1.

Table S1. Definitions and units of model variables.

Symbol	Variable	Unit
M_{Si}	amount of dissolved Si in the lake	[mass]
C_{in}	dissolved Si concentration of inflow	[mass][length]$^{-3}$
t	time	[time]
Q_{in}	discharge into the lake	[length]^3[time]$^{-1}$
Q_{out}	discharge of outflow of the lake	[length]^3[time]$^{-1}$
V	volume of the lake	[length]^3
J	biogenic Si production flux	[mass][time]$^{-1}$
$\delta^{30}\text{Si}_{\text{lake}}$	Si isotope ratios of the lake water	
$\delta^{30}\text{Si}_{\text{in}}$	Si isotope ratios of the inputs	
$\delta^{30}\text{Si}_{\text{bSi}}$	Si isotope ratios of instantaneous growth of diatom	
ε	fractionation factor of diatom growth	
A_{bSi}	amplitude of seasonal variation of diatom growth	
A_{Q}	amplitude of seasonal variation of discharge	
F_{bSi}	frequency of diatom growth	[time]$^{-1}$
F_{Q}	frequency of discharge seasonality	[time]$^{-1}$
τ	time lag between peak discharge and diatom growth	[time]
Q_0	baseline discharge	[length]^3[time]$^{-1}$
J_0	baseline bSi production	[mass][time]$^{-1}$
a	scaling factor in concentration-discharge relationships	
b	exponent in concentration-discharge relationships	
f_{true}	fraction of nutrient remained	
f_{model}	fraction of nutrient remained calculated by an open-system model	

The change of the amount of Si in the lakes over time can be written as Eq. 1:

$$\frac{dM_{\text{Si}}}{dt} = Q_{\text{in}} \cdot C_{\text{in}} - Q_{\text{out}} \cdot \frac{M_{\text{Si}}}{V} - J \tag{1}$$

And Eq. 2 describes the mass balance including isotopes:

$$\frac{d(\delta^{30}\text{Si}_{\text{lake}} \cdot M_{\text{Si}})}{dt} = Q_{\text{in}} \cdot C_{\text{in}} \cdot \delta^{30}\text{Si}_{\text{in}} - Q_{\text{out}} \cdot \frac{M_{\text{Si}}}{V} \cdot \delta^{30}\text{Si}_{\text{lake}} - J \cdot \delta^{30}\text{Si}_{\text{bSi}} \tag{2}$$

For simplicity, we make the assumptions that 1) evaporation is negligible (supported by water isotope measurements of the lakes, Supplementary Figure 1); and 2) lake levels remained relatively constant on seasonal timescales (Eq. 3).

$$Q_{\text{in}} = Q_{\text{out}} \tag{3}$$

At any given instant in time, the Si isotope composition of the growing diatoms should be offset with the lake composition by the fractionation factor (Eq. 4).

$$\delta^{30}\text{Si}_{\text{bSi}} = \delta^{30}\text{Si}_{\text{lake}} + \varepsilon \tag{4}$$

Eqs. 1–2 then rearrange into Eqs. 5–6:

$$\frac{dM_{\text{Si}}}{dt} = Q_{\text{out}} \cdot (C_{\text{in}} - \frac{M_{\text{Si}}}{V}) - J \tag{5}$$

$$\frac{d\delta^{30}\mathrm{Si_{lake}}}{dt} = \frac{Q_{\mathrm{out}} \cdot C_{\mathrm{in}} \cdot (\delta^{30}\mathrm{Si_{in}} - \delta^{30}\mathrm{Si_{lake}}) - J \cdot \varepsilon}{M_{\mathrm{Si}}} \tag{6}$$

where V was estimated from the lake bathymetry and ε is the empirically constrained fractionation factor of diatom growth [6, 7]. We parameterized both discharge (Q_{out}) and diatom growth as sine functions of time (t) with prescribed amplitude (A_{Q}, A_{bSi}) and frequency (F_{Q}, F_{bSi}) to simulate seasonality (Eq. 7 – 8), and the time lag between peak discharge and diatom growth was represented by τ.

$$Q_{\mathrm{out}} = Q_0 \cdot (1 + A_{\mathrm{Q}} \cdot sin(F_{\mathrm{Q}} \cdot t)) \tag{7}$$

$$J = J_0 \cdot (1 + A_{\mathrm{bSi}} \cdot sin(F_{\mathrm{bSi}} \cdot t - \tau)) \tag{8}$$

We assigned the annual average discharge measured at gauges near the lake outlets (V12 and V335, Icelandic Meteorological Office) as the baseline discharge (Q_0) and the average bSi burial flux at each lake as the baseline bSi production (J_0). The Si concentration of river inputs (C_{in}) was related to discharge via the concentration-discharge relationship [8, 9] with scaling factor a and exponent b (Eq. 9). The Si isotope composition of river inputs ($\delta^{30}\mathrm{Si_{in}}$) has been empirically constrained and was held constant over time because $\delta^{30}\mathrm{Si_{in}}$ is expected to be invariant with discharge [10].

$$C_{\mathrm{in}} = a \cdot Q_{\mathrm{in}}^{b} = a \cdot Q_{\mathrm{out}}^{b} \tag{9}$$

We consider the time lag between diatom bloom and peak discharge (τ) to be between 0 – 2 months: the controlling factors of diatom growth (e.g. nutrient delivery, light, and temperature) are correlated with discharge, so the peak growth is expected occur shortly after peak discharge and is unlikely to be temporally decoupled.

The degree of nutrient utilization (f_{true}) can be calculated with integrated J and $Q_{\mathrm{in}} \cdot C_{\mathrm{in}}$ over a year (or a longer time period). Assuming open-system behavior, the fraction of nutrient remaining (f_{model}) can also be calculated with the averaged diatom composition (Eq. 10):

$$\delta^{30}\mathrm{Si_{bSi}} = \delta^{30}\mathrm{Si_{in}} + \varepsilon \cdot f_{\mathrm{model}} \tag{10}$$

Comparing f_{true} and f_{model} then allows us to assess whether the open-system assumption is valid. To account for the uncertainties associated with different parameters, we used a Monte-Carlo approach – 10^4 model simulations were carried out for each lake where (the range of) values chosen for different parameters were specified in Table S2.

Table S2. Model parameters.

Variable	Values (HAK; HVT)	Notes
A_{bSi}	0.1 – 0.9	
A_{Q}	0.1 – 0.9	
F_{bSi}	1 year^{-1}	one bloom per year
F_{Q}	1 year^{-1}	
Q_0	13.4 m^3 s^{-1}; 88.9 m^3 s^{-1}	gauge data (Icelandic Meteorological Office)
J_0	1.6×10^7 mol yr^{-1}; 2.1×10^8 mol yr^{-1}	average burial flux
a	0.9 – 1.6	calibrated with Icelandic rivers [11]
b	-0.15 – -0.05	[8, 9]
τ	0 – 0.15 year	equivalent to 0 – 7.8 weeks

The histograms (as probability density, pdf) of the difference between f_{true} and f_{model} of all model simulations are shown in Supplementary Figure 6. The difference between f_{true} and f_{model} is overall samll, and is less than 5 % in most of the model simulations (94.6% and 93.3% for HAK and HVT, respectively), which supports our parametrization of the lake as an open system.

Text S3: Alternative treatment of diatom growth as closed-system behavior Model results described previously (Text S2) support that the lakes are very likely open systems with respect to diatom growth, i.e. the supply of Si to the lake is always greater than the consumption of Si by diatom growth. Here, we also present calculations of chemical weathering flux under the assumption that the lakes are closed system (i.e. the supply of Si cannot keep pace with the consumption of Si by diatom growth) to account for all possibilities.

The expected Si isotope composition of diatoms ($\delta^{30}\mathrm{Si}_{\mathrm{bSi}}$) can be described with Equation 11 when their growth follows closed-system behavior [12]:

$$\delta^{30}\mathrm{Si}_{\mathrm{bSi}} = \delta^{30}\mathrm{Si}_{\mathrm{initial}} - \varepsilon \cdot \frac{f_{\mathrm{closed}} \cdot ln f_{\mathrm{closed}}}{1 - f_{\mathrm{closed}}} \tag{11}$$

The calculated weathering fluxes are compared against fluxes calculated with an open-system model presented in the main text (Supplementary Figure 7). The calculated fluxes are *systematically* lower when assuming closed-system behavior of diatom growth. Although the absolute weathering fluxes constrained by the two different models are different by almost a factor of 2, the relative changes in weathering fluxes over time and with glacier growth remain the same due to the linear correlation between the fluxes calculated with the two methods. Therefore, in the rare event that the lakes are indeed close systems, our finding that glaciation immediately increases catchment-scale chemical weathering fluxes remains valid.

Text S4: Covariation of riverine δ^{30}Si and Ge/Si during secondary phase formation Central to our approach is the assumption that the correlation between riverine Ge/Si and δ^{30}Si compositions is representative of chemical weathering dynamics in Iceland and remained relatively the same in the past 10 ka, i.e. the apparent sensitivity to the balance between primary mineral dissolution and secondary mineral formation, did not vary.

Compiled δ^{30}Si measurements of glacial and non-glacial rivers in different parts of Iceland [11, 13, 14] show features also observed in our dataset (left panel in Supplementary Figure 8), where glacial rivers share similarly low δ^{30}Si values. This type of first order pattern corroborates the glacial modulation on these chemical signatures and is what we aim to characterize in the regression shown in Figure 2, which should then account for the uncertainty associated with location specific deviations.

The mechanistic control on this correlation is the preferential incorporation of Ge and the lighter Si isotope during secondary phase formation. Riverine Ge/Si ($\text{Ge/Si}_{\text{diss}}$) and δ^{30}Si ($\delta^{30}\text{Si}_{\text{diss}}$) can be calculated with the following equations [15], where $\text{Ge/Si}_{\text{initial}}$ and $\delta^{30}\text{Si}_{\text{initial}}$ are parent rock compositions and f_{solid} is the fraction of total dissolved Si incorporated into secondary phases:

$$\delta^{30}\text{Si}_{\text{diss}} = \delta^{30}\text{Si}_{\text{initial}} - \varepsilon \cdot f_{\text{solid}} \tag{12}$$

$$\text{Ge/Si}_{\text{diss}} = \frac{\text{Ge/Si}_{\text{initial}}}{1 + f_{\text{solid}} \cdot (K_D - 1)} \tag{13}$$

While the Si isotope fractionation factor during secondary phase formation (ε) is relatively well constrained [16, 17, 18], the partition coefficient of Ge into secondary phases (K_D) is poorly known. All existing work points to $K_D > 1$ (see [15] and references therein), however, a wide range up to K_D = 50 [19] has been made. Supplementary Figure 8 show possible theoretical relationships between δ^{30}Si and Ge/Si calculated with variable K_D values, assuming a bedrock composition of $\delta^{30}\text{Si}_{\text{initial}}$ = -0.3 ‰, $\text{Ge/Si}_{\text{initial}}$ = 4, and Si isotope fractionation factor (ε) of -2 ‰. All observations fall within the region defined by K_D = 2 and K_D = 20, but the empirical correlation appears more linear. The linearity likely stems from mixing between river water that experienced different degree of secondary phase formation or that manifested different partition coefficients as a result of other environmental controls. As a result, we opted to use a linear fit to represent this correlation and argue that although the behavior of individual tributaries may vary with time, the averaging effect of mixing will reduce the variability in this inter-catchment correlation.

Text S5: Robustness of the bSi records Our calculations of bSi burial flux and hence the chemical weathering flux rely on previously reported bSi content in the sediments. Therefore, the quality of the bSi records is important. The bSi content in sediments was previously determined by leaching with 10% Na_2CO_3 following protocols described in [20] and published in [5, 21]. As growing evidence suggest the presence of unique Si-containing phases in glacial environments, concerns may arise as to whether these phases bias the bSi records. Although it may be inevitable that some fraction of the non-biogenic phases dissolved during leaching, we believe that this fraction is small and is not biasing the bSi records as discussed in detail below.

The variation of bSi in the sedimentary record is primarily driven by diatom bSi given the observed correlation between total organic carbon (TOC) and bSi (Figure 35 in [22]) and the co-variation between diatom valve density [22] and measured bSi concentration from leaching (Supplementary Figure 9). The trends in valve density and bSi content largely match, despite a slight decoupling between the two since around 2 ka, where the valve density appears low compared to measured bSi content. However, the Si content of diatoms (per cell) calculated from core top measurements is $\sim$24 pmol, still well within the range of Si content reported for freshwater diatoms [23]. Furthermore, diatoms growing under low light intensity are expected to have higher Si content due to low growth rates [24], which is consistent with the elevated ratio of bSi to valve density as glacier growth increased lake turbidity. The four to five orders of magnitude variability in diatom Si content ([23] and references therein) is likely responsible for any deviation between valve density and bSi concentration in the sediment.

Possible non-biogenic Si-phases that may bias leaching are discussed below, and no significant or systematic contributions from these non-biogenic fractions is expected. We would also like to note that no bias was found to associate with different leaching methods when applying to lake sediments [25].

1. Amorphous silica coating on bedrock [26, 27]: it has not been reported for basaltic bedrock and it tends to remain on the rock surface for an extended period of time (persistent enough for U-series dating) and appears to be resistant to weathering.

2. Glacially-derived amorphous silica in river suspended sediments [28, 29, 30, 31]: "aSi" phases only account for up to 1% of Si in total water and sediment discharge (calculated with data presented in [29]), so it's unlikely that this phase is largely biasing the record.

3. Tephra/ash: The presence of ash layers does not correlate with high bSi (Supplementary Figure 9). In [5], the possible impact from diatom burial and amorphous silica from tephra was evaluated and the conclusion was that "Biogenic silica (BSi) in lake sediments primarily comprises diatoms ([32]), although a small contribution may be derived from amorphous silica (glass) of Icelandic volcanic tephra. Analyses of pure tephra levels (no diatoms present) in sediments from a lake in central Iceland suggest that a maximum of 3% of the fine-grained tephra dissolves in the BSi extraction ([22]). Because our sampling specifically avoided tephra levels, we do not expect any significant contribution to our BSi signal from tephra dissolution, even if small amounts of tephra are in the sample."

Text S6: Ge fractionation correction and alternative scenarios considering different diatom Ge uptake behaviors As the uptake and potential discrimination of Ge by freshwater diatoms have not been systematically investigated, the observed Ge/Si offset between lake water and core-top bSi (Figure 2A) at HVT introduces uncertainty in the inference of lake (HVT) δ^{30}Si in the past, which also propagates to our chemical weathering flux calculations. Here, we illustrate how and why this observed offset was corrected during the calculations. We also performed additional calculations under alternative scenarios to test the sensitivity of our results to the assumptions that we made about diatom Ge uptake behaviors. The positive correlation between weathering flux and glacial extent is still observed under these alternative scenarios. Therefore, we consider our main finding to be robust.

The Ge/Si offset between coretop bSi and lake water at HVT suggests discrimination against Ge during diatom growth. The presence of this offset at HVT and the absence of this offset at HAK may be explained by different diatom assemblages inhabiting the lakes. The diatom community at HVT is dominated by planktic species because high turbidity prevents light penetration. The diatom assemblage is likely different at HAK as a result of much lower turbidity. Although we do not have direct observation on the diatom assemblages at HVT, independent constraints indicate a benthic-dominated diatom community when the catchment of HVT is ice free and lake HVT is less turbid [22] (Supplementary Figure 5).

There appears to be a step change in Ge/Si ratios of the bSi samples with time at HVT, where the 3 youngest samples have much lower Ge/Si values (Figure 2A). This change temporally corresponds to a shift from a benthic-dominated to a pelagic-dominated diatom community, most likely due to an increasing supply of sediments and thus turbidity from the expansion of Langjökull glacier between 5 - 3 ka [4] (Supplementary Figure 5). Therefore, an offset from lake Ge/Si could be expected for bSi samples younger than this transition, whereas the older bSi samples should closely record lake Ge/Si, as the diatoms then should share similar Ge and Si uptake pathways as the ones currently inhabiting HAK. It then follows that we apply the observed offset between Ge/Si of modern lake and core-top bSi to the youngest three samples at HVT, while no corrections were made for the older samples (Supplementary Figure 10). This correction also makes sense because the inferred lake Ge/Si then started with lower values $\sim$10 kyr ago and increased over time. As we established earlier that Ge/Si and δ^{30}Si distinguish between glacial and non-glacial catchments (Text S4, Supplementary Figure 8), higher inferred lake Ge/Si at HVT towards the present day suggests that the catchment became "more glacial" in terms of its chemical composition, matching well with the reconstructed glacial history [4].

Although we believe the correction we applied is reasonable given existing observations, we acknowledge that it is ultimately based on assumptions. Therefore, we consider two alternative scenarios and re-calculate the weathering fluxes with different assumptions about diatom behaviors to test the robustness of our results.

First, we assumed that lake δ^{30}Si at HVT has been constant in the past ten thousand years. This would imply that other properties of the catchment outweigh the effect of glaciers over this timescale, and is dominating the lake δ^{30}Si signal. The re-calculated fluxes are quite similar and show the same pattern where weathering flux increases with glacial extent (Supplementary Figure 11 A-B). This is likely because δ^{30}Si of bSi at HVT remained roughtly constant (except the sample at $\sim$ 6 ka) so the reconstructed degree of nutrient utilization ("f") did not vary much and the changes of weathering flux are mostly driven by the changes in bSi burial flux.

Second, we assumed that the behavior of diatom Ge uptake during growth did not change with time at HVT and applied a correction of the same magnitude offset observed at core top for all the bSi samples. Re-calculated fluxes show similar positive correlation with glacial extent (Supplementary Figure 11 C-D). However, we would like to note the caveat that in this scenario the inferred lake Ge/Si and δ^{30}Si suggest the lake water to be "more glacial" in terms of its chemical composition when the catchment was expected to be ice free.

Given that the correlation between weathering fluxes and glacial extent was observed when different assumptions about the lake system and diatom behaviors were made, we conclude that our finding is robust.

In addition, we would like to note that the alternative scenario in which changes in bSi burial are solely driven by changes in the fraction of Si utilization while the weathering flux has been roughly constant is very unlikely. First, our a priori parameter ranges allow for such a scenario, but our Monte Carlo sampling proves it to be improbable. Second, a constant weathering flux would require that the fractional Si utilization has increased substantially over time, which is inconsistent with what we'd expect given how lake temperature, ice cover, and light availability would have changed in response to a cooling climate and the onset of glaciation *while nutrient supply from chemical weathering remained constant*. Specifically, we predict that the onset of glaciation would act to limit diatom productivity via decreases in lake temperature and light penetration (via increases in ice cover and suspended sediment concentrations). Accordingly, we argue that the assumption of a constant weathering flux is an overall unrealistic model for this system given its requirement that the fraction of Si utilization increase as glacial area expands. In our preferred model, the fractional utilization of Si by diatoms has no clear trend with time while Si inputs into the lake increase as glacial cover grows. We think this is an overall more realistic model given modern observations of diatom productivity in Iceland lakes. Specifically, prior work has shown that nutrient inputs, in addition to light availability, influence the seasonal pattern of diatom productivity [33, 34]. So, the increased nutrient supply from glacial weathering could partially offset the effects of increasing ice cover and suspended sediment concentrations, leading to the observation of no significant trend over time (Supplementary Figure 2).

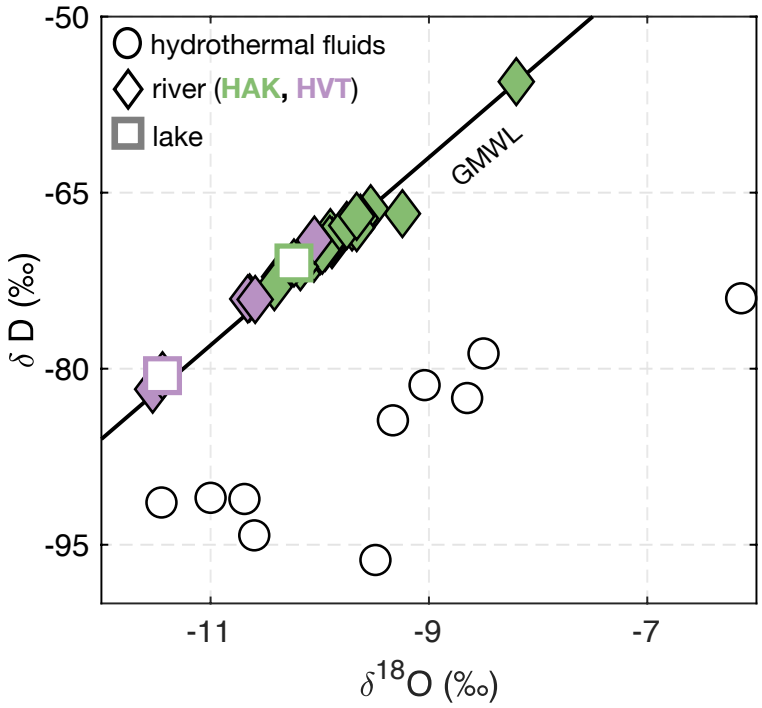

Supplementary Figure 1 δ^{18}O and δD values of all river and lake water samples (normalized to Vienna Standard Mean Ocean Water, VSMOW; error bar smaller than data symbol) lie on the global meteoric water line (GMWL) while the high-temperature (>90 °C) hydrothermal fluids from Geysir and Hveravellir have distinct compositions [35], which suggests minimal hydrothermal input in the catchments studied here and evaporation is negligible in the lakes.

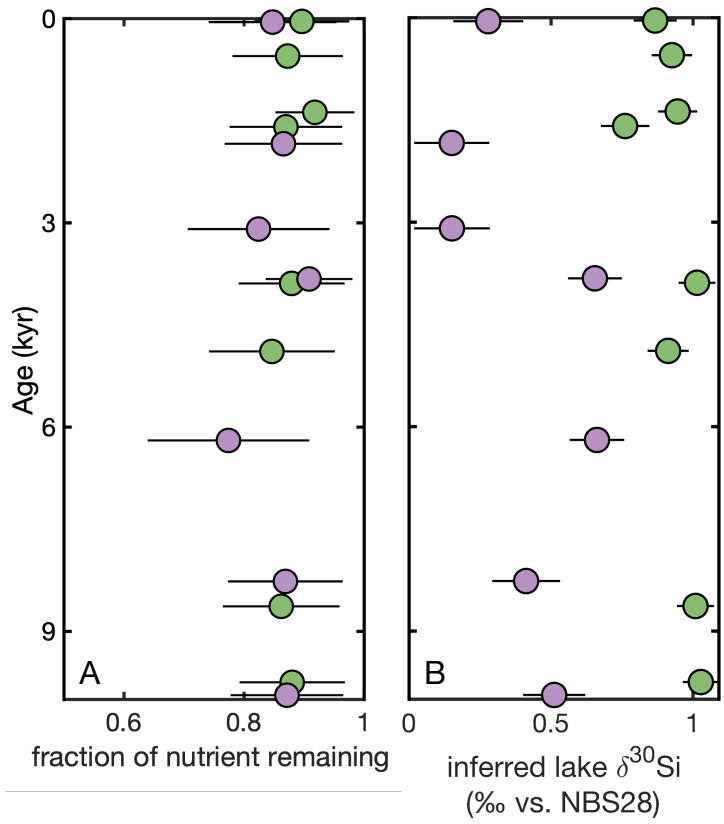

Supplementary Figure 2 Changes in (A) reconstructed fraction of nutrient remaining, (B) inferred lake Si isotopic composition over time.

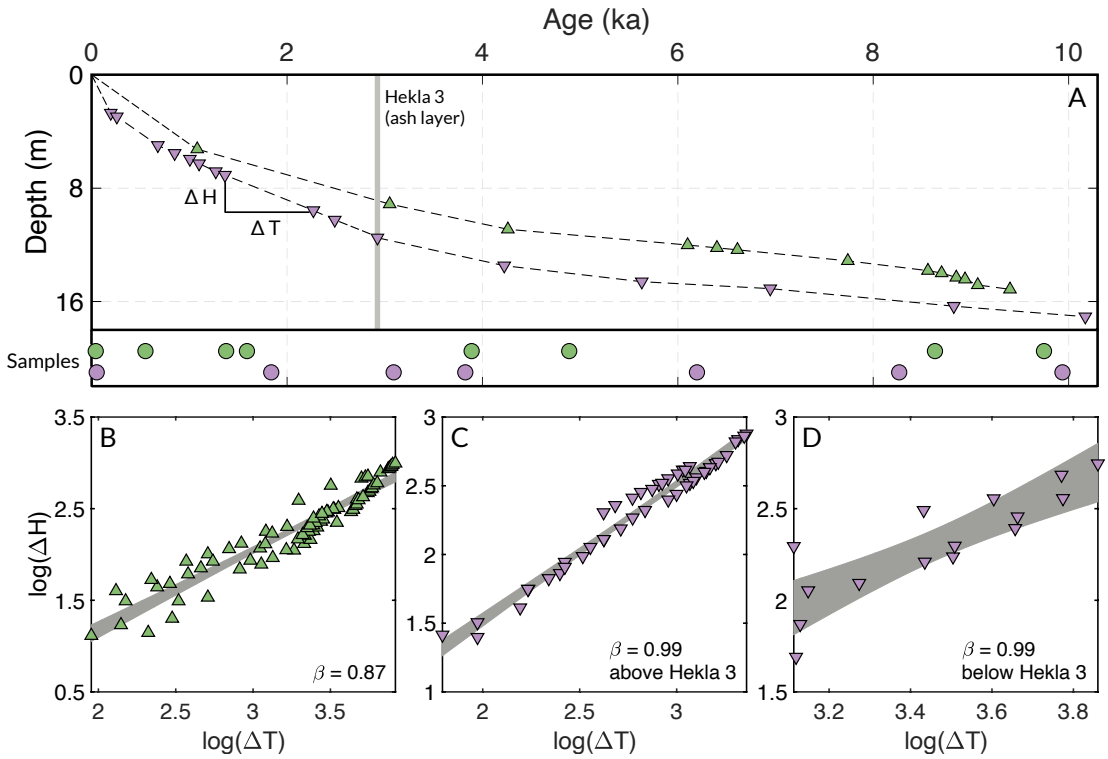

Supplementary Figure 3 (A) Age models of the lake cores, and (B – D) the assessment of the Sadler effect [1, 2] (B – D), where an exponent (β) of 1 indicate that the sedimentary record is unbiased.

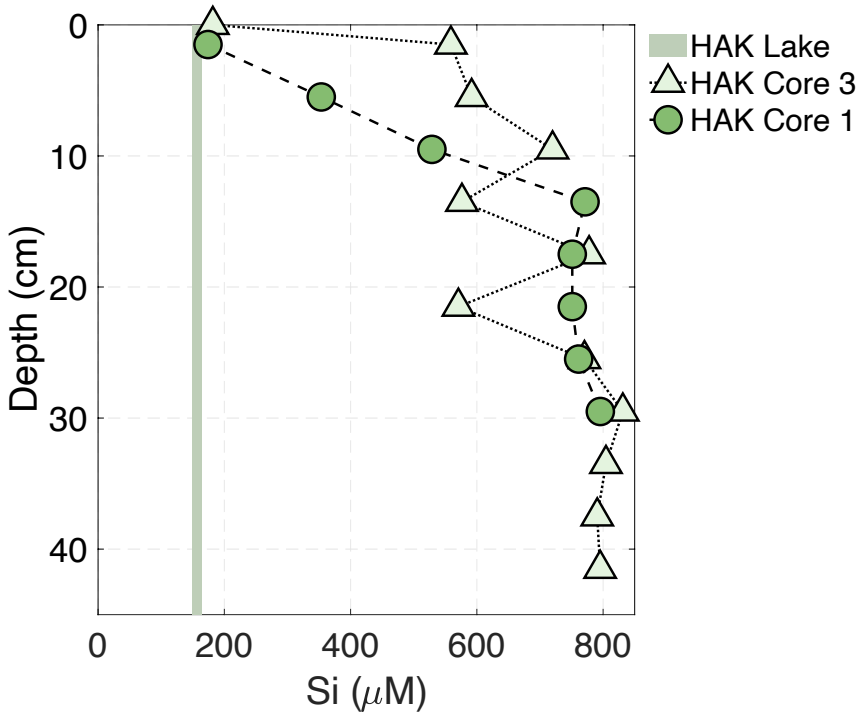

Supplementary Figure 4 Porewater profiles of dissolved Si concentrations from two cores collected in Haukadalsvatn. Dissolved Si concentrations are the same as in the lake at coretop and reach asymptotic values close to amorphous silica saturation at around 15 cm, indicating limited diatom dissolution at higher depth.

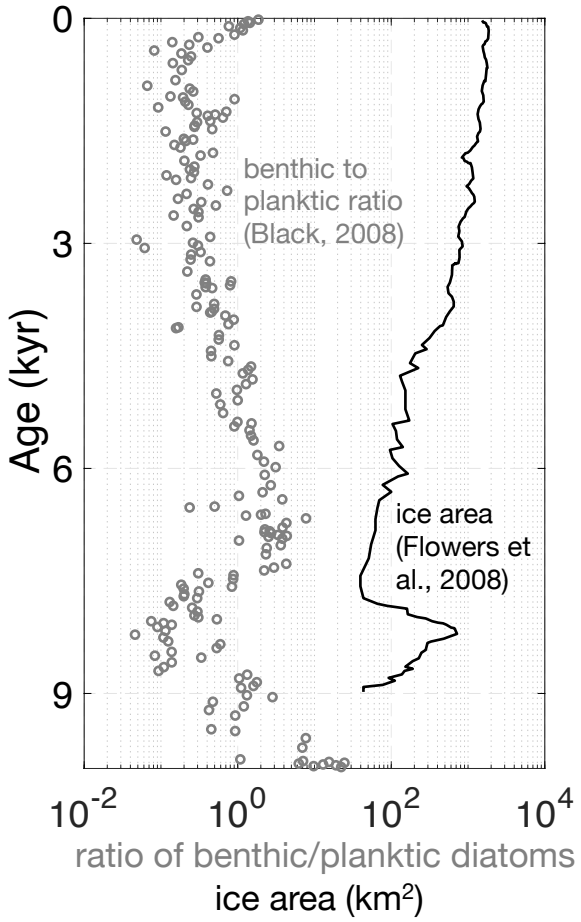

Supplementary Figure 5 Change in diatom community [22] with glacier growth [4] at HVT.

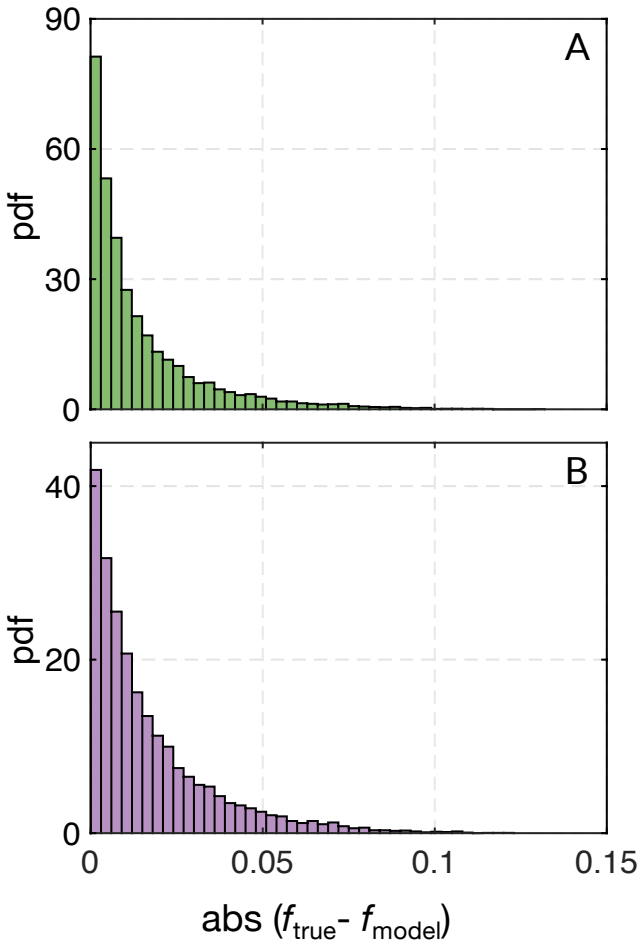

Supplementary Figure 6 Lake model results for HAK(A) and HVT(B). Estimated probability density function of the difference between fraction of nutrient remained calculated by assuming lakes behave as open-systems with Equation 10 (f_{model}), and by integrating numerical solutions to Equations 5–6(f_{true}).

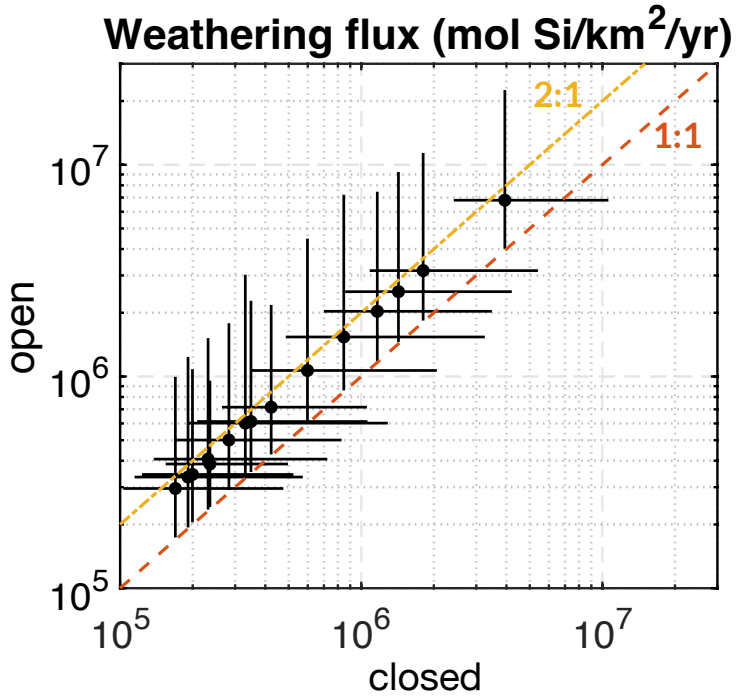

Supplementary Figure 7 Weathering fluxes calculated with a closed-system model compared with the open-system model. Note that 1) the calculated fluxes are consistently lower when assuming closed-system behavior of diatom growth; 2) the weathering fluxes calculated with the different assumptions are positively correlated.

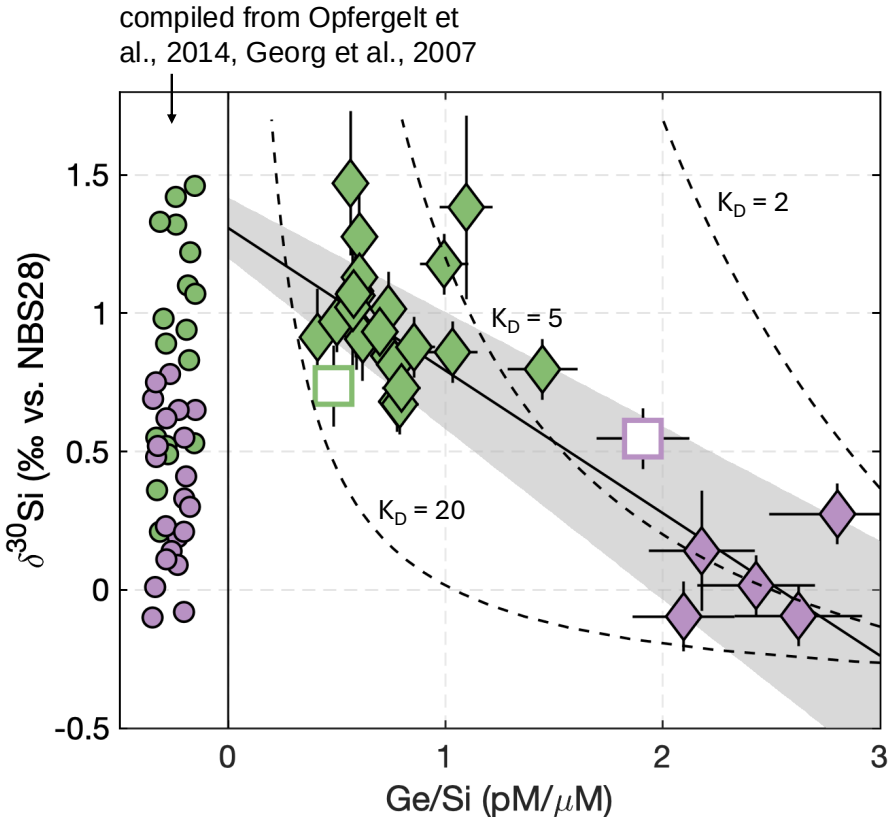

Supplementary Figure 8 Compiled Icelandic river δ^{30}Si measurements (left panel) and theoretical predictions of covariation between river Ge/Si and δ^{30}Si. Dashed lines represent possible correlations given different partition coefficients of Ge into secondary phases (K_D).

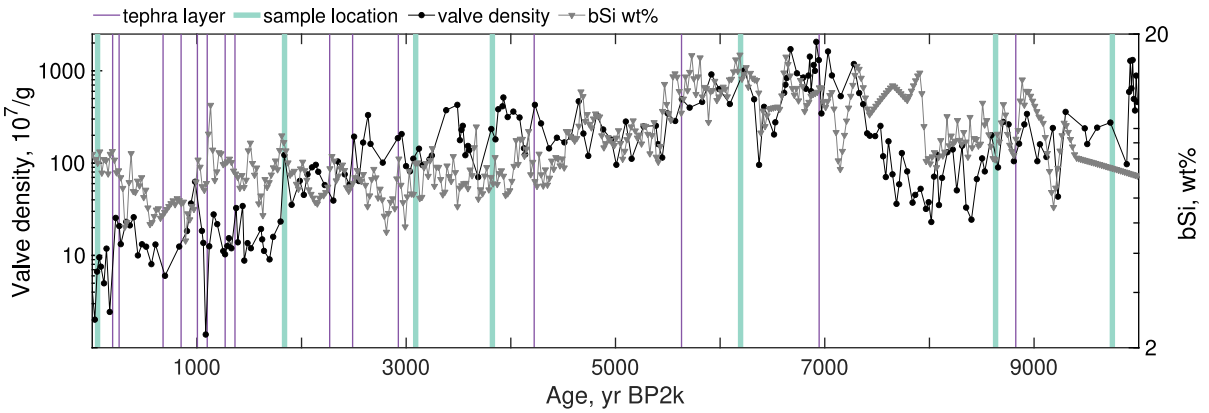

Supplementary Figure 9 Correlation between valve density [22] and bSi concentration (measured by leaching).

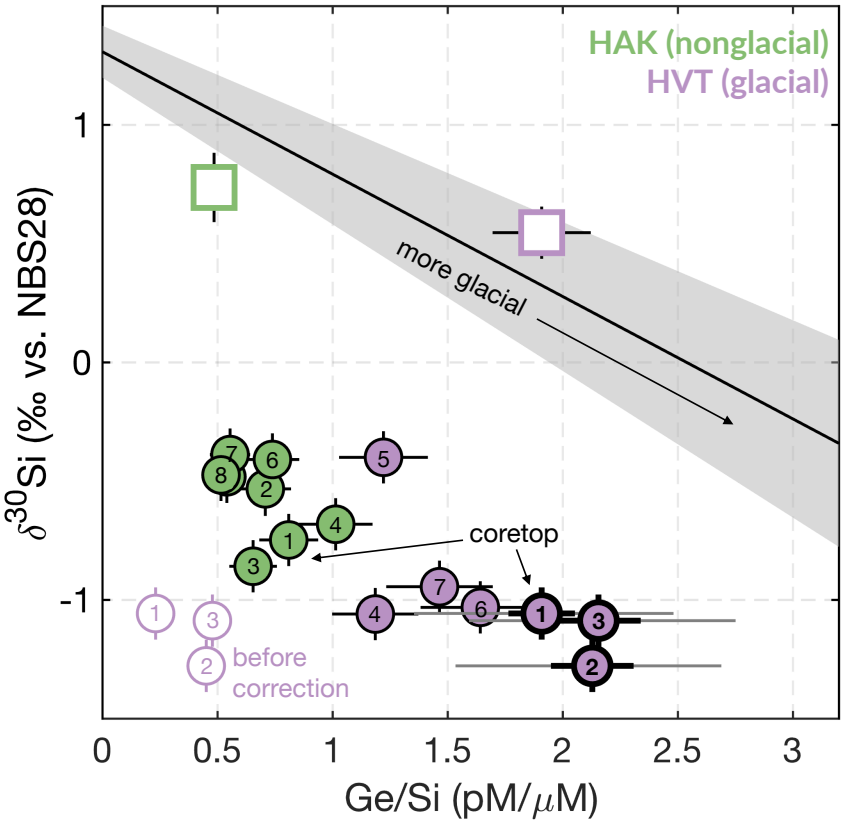

Supplementary Figure 10 Corrections made for the three youngest sedimentary bSi samples in the HVT lake core given the shift of diatom community (benthic to planktic) through time. The grey error bars represent the range of prior used in the calculations and the black error bars represent one standard deviation propagating uncertainty in measured Ge/Si of both bSi and lake water.

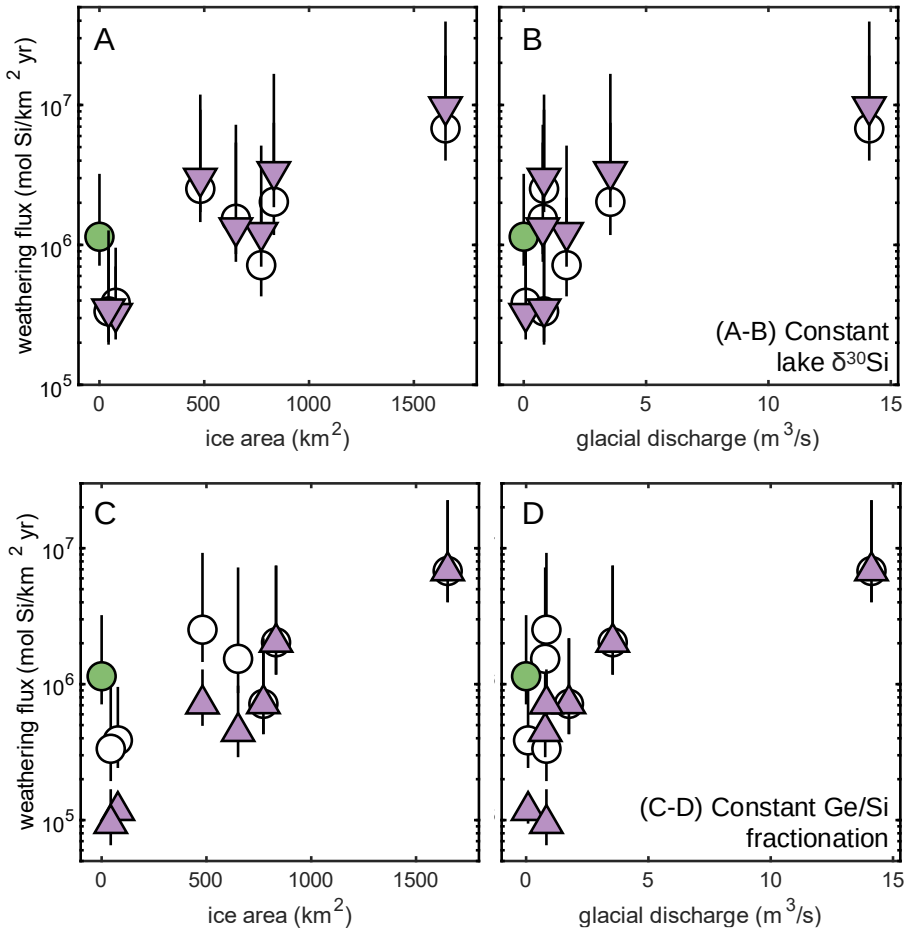

Supplementary Figure 11 Chemical weathering flux as a function of glacial extent (ice area and glacial discharge) with alternative assumptions on Ge fractionation during diatom uptake (see details in Text S6). Panels A-B show results where lake water δ^{30}Si at HVT was considered constant through time. Panels C-D show results where the Ge/Si offset between core-top bSi and lake water was applied to all bSi samples at HVT.

References

[1] P. M. Sadler, "Sediment accumulation rates and the completeness of stratigraphic sections," *The Journal of Geology*, vol. 89, no. 5, pp. 569–584, 1981.

[2] D. J. Jerolmack and P. Sadler, "Transience and persistence in the depositional record of continental margins," *Journal of Geophysical Research: Earth Surface*, vol. 112, no. F3, 2007.

[3] D. J. Larsen, G. H. Miller, Á. Geirsdóttir, and S. Ólafsdóttir, "Non-linear Holocene climate evolution in the North Atlantic: a high-resolution, multi-proxy record of glacier activity and environmental change from Hvítárvatn, central Iceland," *Quaternary Science Reviews*, vol. 39, pp. 14–25, 2012.

[4] G. E. Flowers, H. Björnsson, Á. Geirsdóttir, G. H. Miller, J. L. Black, and G. K. Clarke, "Holocene climate conditions and glacier variation in central Iceland from physical modelling and empirical evidence," *Quaternary Science Reviews*, vol. 27, no. 7-8, pp. 797–813, 2008.

[5] Á. Geirsdóttir, G. H. Miller, T. Thordarson, and K. B. Ólafsdóttir, "A 2000-year record of climate variations reconstructed from Haukadalsvatn, West Iceland," *Journal of Paleolimnology*, vol. 41, pp. 95–115, 2009.

[6] C. L. de La Rocha, M. A. Brzezinski, and M. J. DeNiro, "Fractionation of silicon isotopes by marine diatoms during biogenic silica formation," *Geochimica et Cosmochimica Acta*, vol. 61, no. 23, pp. 5051–5056, 1997.

[7] L. Y. Alleman, D. Cardinal, C. Cocquyt, P.-D. Plisnier, J.-P. Descy, I. Kimirei, D. Sinyinza, and L. André, "Silicon isotopic fractionation in Lake Tanganyika and its main tributaries," *Journal of Great Lakes Research*, vol. 31, no. 4, pp. 509–519, 2005.

[8] S. Moon, C. Chamberlain, and G. Hilley, "New estimates of silicate weathering rates and their uncertainties in global rivers," *Geochimica et Cosmochimica Acta*, vol. 134, pp. 257–274, 2014.

[9] D. E. Ibarra, S. Moon, J. K. Caves, C. P. Chamberlain, and K. Maher, "Concentration–discharge patterns of weathering products from global rivers," *Acta Geochimica*, vol. 36, pp. 405–409, 2017.

[10] J. L. Druhan and P. Benettin, "Isotope ratio–discharge relationships of solutes derived from weathering reactions," *American Journal of Science*, vol. 323, p. 5, 2023.

[11] T. L. Cole, M. A. Torres, and P. C. Kemeny, "The hydrochemical signature of incongruent weathering in Iceland," *Journal of Geophysical Research: Earth Surface*, vol. 127, no. 6, p. e2021JF006450, 2022.

[12] D. E. Varela, C. J. Pride, and M. A. Brzezinski, "Biological fractionation of silicon isotopes in Southern Ocean surface waters," *Global Biogeochemical Cycles*, vol. 18, no. 1, 2004.

[13] S. Opfergelt, K. Burton, P. P. Von Strandmann, S. Gislason, and A. Halliday, "Riverine silicon isotope variations in glaciated basaltic terrains: Implications for the si delivery to the ocean over glacial–interglacial intervals," *Earth and Planetary Science Letters*, vol. 369, pp. 211–219, 2013.

[14] R. Georg, B. C. Reynolds, A. West, K. Burton, and A. N. Halliday, "Silicon isotope variations accompanying basalt weathering in Iceland," *Earth and Planetary Science Letters*, vol. 261, no. 3-4, pp. 476–490, 2007.

[15] P. J. Frings, F. Schubring, M. Oelze, and F. von Blanckenburg, "Quantifying biotic and abiotic Si fluxes in the Critical Zone with Ge/Si ratios along a gradient of erosion rates," *American Journal of Science*, vol. 321, no. 8, pp. 1204–1245, 2021.

[16] K. Ziegler, O. A. Chadwick, M. A. Brzezinski, and E. F. Kelly, "Natural variations of δ30si ratios during progressive basalt weathering, hawaiian islands," *Geochimica et Cosmochimica Acta*, vol. 69, no. 19, pp. 4597–4610, 2005.

[17] S. Delstanche, S. Opfergelt, D. Cardinal, F. Elsass, L. André, and B. Delvaux, "Silicon isotopic fractionation during adsorption of aqueous monosilicic acid onto iron oxide," *Geochimica et Cosmochimica Acta*, vol. 73, no. 4, pp. 923–934, 2009.

[18] M. Méheut and E. A. Schauble, "Silicon isotope fractionation in silicate minerals: Insights from first-principles models of phyllosilicates, albite and pyrope," *Geochimica et Cosmochimica Acta*, vol. 134, pp. 137–154, 2014.

[19] A. Perez-Fodich and L. A. Derry, "A model for germanium-silicon equilibrium fractionation in kaolinite," *Geochimica et Cosmochimica Acta*, vol. 288, pp. 199–213, 2020.

[20] R. A. Mortlock and P. N. Froelich, "A simple method for the rapid determination of biogenic opal in pelagic marine sediments," *Deep Sea Research Part A. Oceanographic Research Papers*, vol. 36, no. 9, pp. 1415–1426, 1989.

[21] Á. Geirsdóttir, G. H. Miller, D. J. Larsen, and S. Ólafsdóttir, "Abrupt Holocene climate transitions in the northern North Atlantic region recorded by synchronized lacustrine records in Iceland," *Quaternary Science Reviews*, vol. 70, pp. 48–62, 2013.

[22] J. L. Black, *Holocene climate change in south-central Iceland: A multi-proxy lacustrine record from glacial lake Hvítárvatn*. PhD thesis, University of Colorado at Boulder, 2008.

[23] D. J. Conley, S. S. Kilham, and E. Theriot, "Differences in silica content between marine and freshwater diatoms," *Limnology and oceanography*, vol. 34, no. 1, pp. 205–212, 1989.

[24] N. Taylor, "Silica incorporation in the diatom cosinodiscus granii as affected by light intensity," *British Phycological Journal*, vol. 20, no. 4, pp. 365–374, 1985.

[25] L. Barao, F. Vandevenne, W. Clymans, P. Frings, O. Ragueneau, P. Meire, D. J. Conley, and E. Struyf, "Alkaline-extractable silicon from land to ocean: A challenge for biogenic silicon determination," *Limnology and Oceanography: Methods*, vol. 13, no. 7, pp. 329–344, 2015.

[26] T. Blackburn, S. Siman-Tov, M. A. Coble, G. M. Stock, E. E. Brodsky, and B. Hallet, "Composition and formation age of amorphous silica coating glacially polished surfaces," *Geology*, vol. 47, no. 4, pp. 347–350, 2019.

[27] S. Siman-Tov, T. Blackburn, B. Hallet, M. A. Coble, and E. E. Brodsky, "Siliceous subglacial deposits: archives of subglacial processes during the last glacial maximum," *Journal of Glaciology*, vol. 67, no. 266, pp. 977–984, 2021.

[28] J. E. Hatton, K. R. Hendry, J. R. Hawkings, J. L. Wadham, S. Opfergelt, T. J. Kohler, J. C. Yde, M. Stibal, and J. D. Žárskỳ, "Silicon isotopes in arctic and sub-arctic glacial meltwaters: the role of subglacial weathering in the silicon cycle," *Proceedings of the Royal Society A*, vol. 475, no. 2228, p. 20190098, 2019.

[29] J. Hatton, K. Hendry, J. Hawkings, J. Wadham, T. Kohler, M. Stibal, A. Beaton, E. Bagshaw, and J. Telling, "Investigation of subglacial weathering under the greenland ice sheet using silicon isotopes," *Geochimica et Cosmochimica Acta*, vol. 247, pp. 191–206, 2019.

[30] J. Hatton, K. Hendry, J. Hawkings, J. L. Wadham, L. G. Benning, R. Blukis, V. Roddatis, H. C. Ng, and T. Wang, "Physical weathering by glaciers enhances silicon mobilisation and isotopic fractionation," *Geochemical Perspectives Letters*, vol. 19, pp. 7–12, 2021.

[31] J. R. Hawkings, J. L. Wadham, L. G. Benning, K. R. Hendry, M. Tranter, A. Tedstone, P. Nienow, and R. Raiswell, "Ice sheets as a missing source of silica to the polar oceans," *Nature communications*, vol. 8, no. 1, p. 14198, 2017.

[32] D. J. Conley and C. L. Schelske, "Biogenic silica," *Tracking environmental change using lake sediments: terrestrial, algal, and siliceous indicators*, pp. 281–293, 2001.

[33] S. Opfergelt, E. Eiriksdottir, K. Burton, A. Einarsson, C. Siebert, S. Gislason, and A. Halliday, "Quantifying the impact of freshwater diatom productivity on silicon isotopes and silicon fluxes: Lake Myvatn, Iceland," *Earth and Planetary Science Letters*, vol. 305, no. 1-2, pp. 73–82, 2011.

[34] P. M. Jónasson, H. Adalsteinsson, and G. St. Jónsson, "Production and nutrient supply of phytoplankton in subarctic, dimictic Thingvallavatn, Iceland," *Oikos*, pp. 162–187, 1992.

[35] S. Arnórsson, "The use of mixing models and chemical geothermometers for estimating underground temperatures in geothermal systems," *Journal of Volcanology and Geothermal Research*, vol. 23, no. 3-4, pp. 299–335, 1985.